INTRACELLULAR LOCALIZATION AND QUANTIFICATION OF HYDROGEN SULFIDE AND NITROGEN DIOXIDE

SAARANGAN KRISHNAKUMAR

NATIONAL UNIVERSITY OF SINGAPORE

2014

INTRACELLULAR LOCALIZATION AND QUANTIFICATION OF HYDROGEN SULFIDE AND NITROGEN DIOXIDE

SAARANGAN KRISHNAKUMAR

(B. Tech., Anna University)

A THESIS SUBMITTED

FOR THE DEGREE OF MASTER OF SCIENCE

DEPARTMENT OF CHEMISTRY

NATIONAL UNIVERSITY OF SINGAPORE

2014

Declaration Page

I hereby declare that this thesis is my original work and it has been written by me in its entirety, under the supervision of Associate Professor Huang Dejian (in the laboratory S13-05-02), Department of Chemistry and Assistant Professor Deng Lih Wen (in the lab MD6, Level 14), Department of Biochemistry, National University of Singapore between August 2012 and April 2014.

I have duly acknowledged all the sources of information which have been used in the thesis.

This thesis has also not been submitted for any degree in any university previously.

The content of the thesis has been partly published in:

1. *Journal of American Chemical Society*, 2013, 135, 5312-5315.
2. *Chemistry Asian Journal, 2014,* 9, 3604-3611.

_____	_____	_____
Name	Signature	Date

Acknowledgements

Firstly, I would like to express my deepest sense of gratitude to my supervisor, Assoc. Prof. Huang Dejian, for his valuable advice, constructive and critical comments and extensive discussions around my work. I am very much grateful to him in every possible way for giving me this opportunity to work under his excellent personal guidance and for his expert assistance, which has been absolutely helpful and essential for completion of this thesis. I owe him a lot.

Secondly, I am greatly indebted to my co-supervisor, Dr. Deng Lih-Wen for her extensive guidance and mentoring. I feel honored to have her as my guide and was honored to learn invaluable ideas, profound knowledge and rich research experience. Words are due to express my sincere gratitude, as this thesis in its present form is only due to her extensive help, constant support and encouragement.

I would like to thank Dr. Yan Yan and Dr. Wu Haixia for synthesis of fluorescent probes and their constant support and technical assistance rendered throughout the project. I also thank Mr. Lee Zheng Wei, Mr. Zhao Wei for their support in cell culture and molecular biology techniques. I would also like to extend my appreciation to Ms. Lee Shu Ying for aiding me in gaining technical expertise in advanced microscopy techniques and image processing.

I would also like to appreciate Ms. Lee Chooi Lan, Ms. Lew Huey Lee, Ms. Jiang Xiaohui for their excellent technical assistance. I would also like to express my heartfelt appreciation to Mr. Mukundarajan, , Dr. Devanathan Raghunathan, Mr. Mugunthan Gopal, Mr. Arun Thiyagarajan and Mr. Hari Krishnan for their constant support and personal advice.

I would also extend my deepest gratitude to my family members for their love and unwavering support throughout Master's study. I also thank all my friends whose name may not have been mentioned here, but have never hesitated to give me their helping hands whenever I need help.

Above all I thank the “Almighty” for all the blessings and guiding me throughout this two years of study.

Saarangan Krishnakumar

September 2014

Table of Contents

Summary

Detection of small gaseous molecules of biological importance have been carried out in the past using various techniques including colorimetry, electron paramagnetic resonance, electrochemistry, gas chromatography, metal-induced sulfide precipitation. Whereas the fluorescent probe based detection has many advantages such as high sensitivity, selectivity and versatility to yield information about the gaseous molecules. To couple with the quantitative information obtained using fluorescent probes, high quality confocal imaging was carried out to unravel the intracellular localization of the gaseous molecules.

This study was based on the two fluorescent probes namely Ni(II) dithiocarbamate complex based fluorescent probe sensitive towards nitrogen dioxide (NO_2) and BODIPY-Cyclen (BDP-Cy) based fluorescent probe sensitive towards hydrogen sulfide (H_2S). Both these probes are hydrophobic in nature, hence a cationic liposome mediated delivery method was utilised for subcellular detection. The NO_2 specific probe was investigated in cellular environment to unravel the fate of nitric oxide (NO, known gaseous messenger). The external NO donor namely DEANO was administered in RAW 264.7 cells to determine the formation of NO_2 due to the rapid reaction NO and oxygen in the cellular system. The positive results allowed us to further look into endogenously produced NO_2 using inducible Nitric Oxide Synthase (iNOS) pathway. Lipopolysaccharides (LPS) was used as stimulant and increase in fluorescent intensity was observed with increase in stimulation time. These results were in accordance to previous results suggesting a possible conversion of NO produced in the cell to NO_2.

The H_2S specific probe was analysed for its selectivity and sensitivity in RAW 264.7 cells using external donors such as Na_2S and NaHS. A dose dependent increase in fluorescent intensity was observed, which allowed us to further monitor the endogenous H_2S in HEK 293 cells by using gene knockdown and overexpression of inherent cystathionine γ-lyase (CSE) gene. The fluorescent probe was further applied in determining the H_2S produced by natural and synthetic polysulfides in MCF-7 cells. Finally, a combination of NO_2 sensitive probe and H_2S sensitive probe was utilised in analysing the quenching activity of H_2S on nitrogen radicals.

List of Tables

List of Figures

Figure 2.3 Cytotoxicity data for DOTAP at various concentrations after 4 h incubation with RAW 264.7 cells. The DOTAP at 100 μM adopted in the cell imaging experiment demonstrates negligible cytotoxicity (less than 5%).

Figure 2.4 Cytotoxicity data for probe 1 and probe 2 at various concentrations after 4 h incubation with RAW 264.7 cells. The concentrations of probe at 5μM and 3 μM adopted in the cell imaging experiment demonstrates negligible cytotoxicity (less than 2%).

Figure 2.5 NO_2 turns on the fluorescence of RAW 264.7 cells stained with probe 1 (A) and (B) are 3D images of single cell not treated and treated with DEANO (1 mM) respectively.(C) and (D) are 3D images group of cells not treated and treated with DEANO (1 mM) respectively, together with their respective white field cell images.(E) Confocal fluorescent microscopes of cells treated with different concentrations of DEANO (0, 0.2, 0.5, 1 mM) and their respective white field cell images. (F) Fluorescence quantification of confocal images of RAW 264.7 cells stained with probe 1, with and without DEANO treatment (n = 5).

Figure 2.6 Detection of NO2 in RAW 264.7 cells by DOTAP-probe 2 mixture. The top images are 3D fluorescent images and bottom images are corresponding 2D DIC images. Cells a) treated with DOTAP-probe 2 mixture (3 μM) for 2 hours b) pre-stimulated with LPS (2 μg/ml) for 16 hours and treated with DOTAP-probe 2 mixture(3 μM) for 2 hours. c) sequentially treated with L-NAME(0.5mM) for 2 hours, LPS (2 μg/ml) for 16 hours and DOTAP-probe 2 mixture(3 μM) for 2 hours. d) incubated with DOTAP-probe2 mixture(3 μM) for 2 hours and DEANO (1mM) for 10 min. (B) Fluorescence quantification of confocal images of RAW 264.7 cells stained with the probe 2 for various treatments using imageJ software (n = 10).

Figure 2.7 Endogenous NO_2 detection in RAW 264.7 cells by probe 2-DOTAP mixture. The upper panel is fluorescent images and the lower panel is corresponding bright-field images. The cells were

treated with probe 2-DOTAP mixture (3 μM) for 2 h, then with LPS pre-stimulation (2 μg/ml) for 0, 8, 12 and 16 h, respectively.

Figure 3.1 Molecular structure of diallyl disulfide and diallyl trisulfide.

Figure 3.2 Molecular structure of GYY 4137 and FW 1010.

Figure 3.3 Cytotoxicity data for probe 3 at various concentrations after 4 h incubation with RAW 264.7 cells. The concentration of probe at 10μM adopted in the cell imaging experiment demonstrates negligible cytotoxicity (less than 2%).

Figure 3.4 Detection of H_2S in RAW 264.7 cells. The probe 3(10 μM) in RAW 264.7 was specifically turned on by H_2S contributed by Na_2S (25 μM) but not the other thiol-containing molecules such as cysteine (2 mM) or glutathione (2 mM).

Figure 3.5 Exogenous H_2S detection in RAW 264.7 cells by probe 3. The upper panel is the fluorescent images and lower panel is corresponding bright field images. The cells were treated with probe 3 in DOTAP liposome (10 μM) for 1 hour and Na_2S(0, 25, 50, 100, 150 and 200μM) for 30min respectively. The images were quantified using imageJ for dose response of H_2S concentration and fluorescence intensity(n = 12).

Figure 3.6 Fluorescent and corresponding bright field images of diallyl disulphide treatement in MCF-7 cells. The cells were treated with probe 3 in DOTAP liposome followed by NaHS 400 μM, DADS 100 μM, DADS 200 μM and GSH 1mM + DADS 200 μM. Non-treated cells acted as control.

Figure 3.7 Fluorescent and corresponding bright field images of diallyl trisulfide (DATS) treatement in MCF-7 cells. The cells were treated with probe 3 in DOTAP liposome followed by NaHS 400 μM, DATS 100 μM, DATS 200 μM and GSH 1mM + DATS 200 μM. Non-treated cells acted as control.

Figure 3.8 Fluorescent and corresponding bright field images of GYY 4137 and FW 1010 treatment in MCF-7 cells. The cells were treated with probe 3 in DOTAP liposome followed by NaHS (100, 200 and 400 μM) GYY4137 (400 μM, 800 μM) and FW1010 (400 μM, 800 μM) Non-treated cells acted as control. The images were quantified using imageJ for fluorescence intensity plot(n = 10).

Figure 3.9 Fluorescence microscopy pictures showing signals in cells with manipulated expression of endogenous H_2S-producing enzymes, cystathionine-γ lyase (CSE). Overexpression of wild-type (WT) CSE in HEK293 cells showed increased fluorescence intensity as compared to scrambled control (SC) and CSE knock-down (KD). Hyperactive E339A mutant showed even enhanced fluorescence signal than WT.

Figure 4.1 Cytotoxicity data for combined probe at various concentrations after 4 h incubation with RAW 264.7 cells. The concentration of probe adopted in the cell imaging experiment demonstrates negligible cytotoxicity (less than 2%).

Figure 4.2 Fluorescent imaging of NO_2-H_2S by combined probe- DOTAP mixture. The upper panel is fluorescent images and the lower panel is corresponding bright-field images. Cells a) treated with DOTAP- combined probe solution for 2 hours b) pre-stimulated with LPS (2 μg/ml) for 16 hours and treated with combined probe solution for 2 hours. c) Sequentially treated with LPS (2 μg/ml) for 16 hours, DOTAP- combined probe solution for 2 hours and Na_2S(200 μM) for 30 min. d) incubated with DOTAP- combined probe solution for 2 hours and Na_2S (200 μM) for 30 min.

Figure 4.3 Fluorescent and corresponding bright field images of NO_2- H_2S in RAW 264.7 cells. The cells were a) treated with DOTAP-combined probe solution for 2 hours. b) pre-stimulated with LPS (2 μg/ml) for 16 hours and treated with combined probe solution for 2 hours. c) DOTAP- combined probe solution for 2 hours and Na_2S (200 μM) for 30 min. d) H_2S and NO_2 images are separately monitored in sequential treatment of LPS (2 μg/ml) for 16 hours, DOTAP- combined probe solution for 2 hours and Na_2S(50 μM), e) Na_2S(100 μM), f) Na_2S(200 μM) for 30 min.

Figure 4.4 Fluorescent and corresponding bright field images of time based scanning of NO_2- H_2S intertalk in RAW 264.7 cells. The cells were a) treated with DOTAP- combined probe solution for 2 hours. b) pre-stimulated with LPS (2 μg/ml) for 16 hours and treated with combined probe solution for 2 hours. c) DOTAP- combined probe solution for 2 hours and Na_2S(200 μM) for 30 mins. d) under NO_2 laser slit alone open followed by sequential treatment with LPS (2 μg/ml) for 16 hours, DOTAP- combined probe solution for 2 hours and Na_2S(200 μM) for 30 mins. e) under the H_2S laser slit alone open and same treatment as d).

List of Abbreviations

Abbreviation	Description
BODIPY	boron-dipyrromethene
DEANO	diethylamine NONOate
DMEM	Dulbecco's modified Eagle's medium
DOTAP	1,2-dioleoyl-3-trimethylammonium-propane chloride salt
FRET	Förster resonance energy transfer
HPLC	high performance liquid chromatography
iNOS	inducible nitric oxide synthases
IUPAC	International Union of Pure and Applied Chemistry
LDH	lactate dehydrogenase
L-NAME	L-NG-nitroarginine methyl ester
LOD	limit of detection
LOQ	limit of quantitation
LPS	lipopolysaccharides
MLCT	metal-to-ligand charge transfer
NAD	nicotinamide adenine dinucleotide
NADP	nicotinamide adenine dinucleotide phosphate
NOSs	nitric oxide synthases
PBS	phosphate buffered saline
Ach	Acetylcholine
EDRF	endothelium-derived relaxing factor
IFN- γ	interferon-γ
TNF- α	tumor necrosis factor-α

FBS	fetal bovine serum
GYY 4137	4-methoxyphenyl(morpholino) phosphinodithiolate
FW 1010	4-methoxyphenyl phosphinodithiolate
GSH	glutathione reduced
Cys	Cysteine
DCM	dichloremethane
MCF-7	Michigan Cancer Foundation-7 cells
HEK 293	Human Embryonic kidney 293
RAW 264.7	Mouse leukaemic murine macrophage cells
DADS	diallyl disulfide
DATS	diallyl trisulfide
ICT	intramolecular charge transfer
DNA	deoxyribonucleic acid
PDA	photodiode array
PET	photo-induced electron transfer
QY	quantum yield
RNS	reactive nitrogen species
ROS	reactive oxygen species
SOD	superoxide dismutase
SRB	sulforhodamine B
RhoB	rhodamine B
WT	Wild-type mutated HEK 293 cells
HNO	nitroxyl
HSNO	nitrosothiol

Chapter 1. Introduction: Intracellular Detection of Small Gaseous Molecules by Fluorescent Probes

1.1 Gaseous messengers

1.1.1 General introduction of gaseous messengers

Small molecules of endogenous gases which involve in cellular signaling thereby exerting physiological functions are termed as gaseous messengers or gasotransmitters. Gasotransmitters are a class above the receptor based signaling molecules as they are easily permeable across membranes and directly interact with their intracellular targets.[1,2] Nitric oxide (NO), Carbon monoxide (CO) and Hydrogen sulfide (H_2S) are the enzymatically produced gases with biological functions to maintain the cellular homeostasis.[3]

NO was the first discovered gaseous messenger for its regulatory activity in the vascular system and further research led to its role in immune system and nervous system. The research on physiological activity of NO in vascular system also aided in understanding the effect of carbon monoxide in vasodilation and synaptic cleft.[4,5] Whereas, H_2S is the latest addition for its noted role in cardiovascular and nervous system.[6] Certain other gases such as NH_3, acetaldehyde may also come under the class of gasesous messengers with more concluding evidence. It is to be noted that under specific cellular environments, gasotransmitters can also play a inhibitory role to the physiological functioning.[7] The physiological activity exerted by these gases at micromolar concentrations limits the toxic and hazardous nature. The increase in levels of NO can lead to the formation of oxidative reactive nitrogen species (RNS) that degrade the cellular biomolecules. At higher levels, CO can reduce the oxygen carrying capacity of hemoglobin by forming carboxyhemoglobin. Recently, abnormal levels of H_2S was associated with Alzheimer's disease. [8,9,10] It is evident that the physiological levels of gasotransmitters play a pivotal role in their normal function and abnormal

levels can have delirious pathological effects such as neurodegeneration, carcinogenesis and ageing related disorders.

1.1.2 Nitric Oxide

In 1980, the relaxation of rabbit aorta by acetylcholine (ACh) required a release of endothelium-derived relaxing factor (EDRF) from endothelium. In the coming years, the pharmacological nature of EDRF was found to be similar to that of NO and further its role in other cells were investigated.[11] In cells, nitric oxide is synthesised by three isoforms of nitric oxide synthase(NOS): neuronal NOS (nNOS or NOS I); inducible NOS (iNOS or NOS II); endothelial NOS (eNOS or NOS III). NOS catalyzes the reaction that produces NO and L-citrulline from L-arginine and O_2 precursors. The structure of NOS proteins are similar among three distinct domains: *N*-terminal oxygenase domain, a calmodulin binding domain and a *C*-terminal reductase domain. Both eNOS and nNOS are calcium-dependent and are activated by an increase in intracellular calcium (Ca^{2+}). Whereas iNOS is an external stimuli dependent NOS which catalyzes the conversion of L-arginine to L-citrulline and NO. Endotoxins like lipopolysaccharides (LPS) and cytokines such as Interferon-γ (IFN- γ), Tumor necrosis factor-α (TNF-α) act as the external stimulant.[12,13]

In contrast to other two types of NOS proteins which are specific to endothelial and neural cells, iNOS is found in a variety of cells such as phagocytic leukocytes, chondrocytes, astrocytes, heaptocytes and macrophages. The unique property of iNOS is the activated calmodulin subunit, thereby making the production of NO independent of intracellular Ca^{2+} level. Maximum level of NO production is reached 24 hours after

induction by external stimuli and recedes dramatically. The main role of NO in macrophages is to enable cell death mediated by cytotoxic agents against invading organisms. But the excess production of NO can also act as a precursor for production of reactive nitrogen species (RNS) and reactive oxygen species (ROS) leading to cell death.

1.1.3 Presence of Nitric oxide, Nitrites and Nitrates in cellular environment

NO is well known for its wide variety of physiological regulation in blood pressure, neuronal signaling and neutrophil aggregation. In presence of sufficient molecular oxygen, NO reacts spontaneously to form NO_2, which is coupled with NO to give N_2O_3, a reaction intermediate believed having deleterious effect on DNA by nitrosation of primary amines.[71,72] NO can react with superoxide (O_2^-) to form peroxynitrate ($ONOO^-$), an important RNS causing cellular and mutagenic damages. Further cellular level studies are

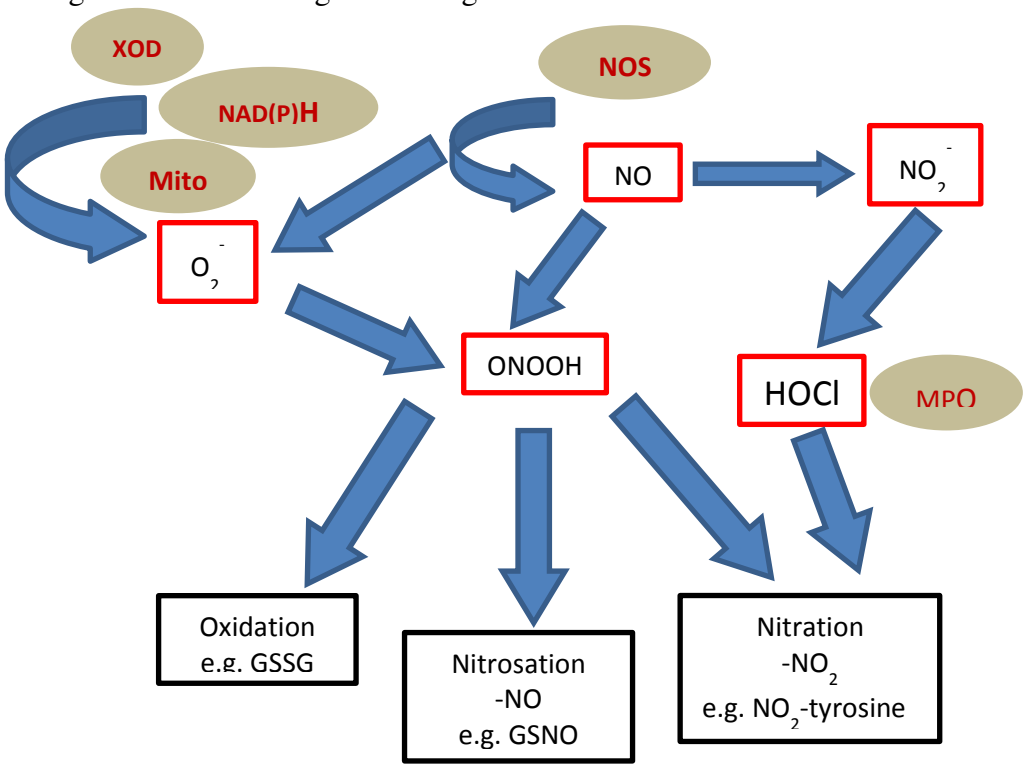

Figure 1.1 Reactive Nitrogen Species (RNS) production and physiological effects.

are needed in order to understand the availability of NO and the rate of conversion into nitrites and nitrates.[15]

RNS is a term profoundly used in scientific reports, they are group of molecules which may contain free radicals and non-radical species that can alter physiological cell signaling or have pathological effects. (Fig 1.1)

$NO^{\cdot}$ gets oxidized to form the subsequent productssuch as nitrogen dioxide (NO_2), nitrite (NO_2^-), these molecules in-turn react with other radicals to form RNS such as peroxynitrite ($ONOO^-$) and peroxynitrous acid (ONOOH). The LPS induced iNOS pathway elucidated the oxidative mechanism of NO andunravelled the skeleton for the existence of nitrites and nitrates produced in the cell.[17]

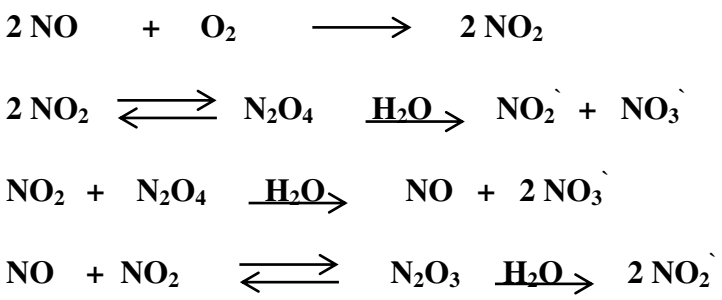

Figure 1.2 Reaction mechanism of production of nitrites and nitrates.

Experiments involving oxygen depleted conditions showed the presence of NO alone, but under normal cellular environment production of NO, NO_2^-, and NO_3^- was validated. (Fig 1.2) The L-arginine provides the nitrogen atom implying that NO acts as an intermediate product in the production of NO_2^- and NO_3^-. The fate of NO and its oxidation products is still unclear on both the pathological and physiological facets and selective detection of NO_2^- using fluorescent probes might aid in the process.[18]

1.1.4 Hydrogen sulfide

For hundreds of years, hydrogen sulfide (H_2S) has been known as a toxic pollutant. But in the past decade, the opinion has changed from noxious gas to gasotransmitter.[92] It is colorless and highly soluble in water but also in lipophilic solvents, thereby all allowing it to diffuse through cell membranes and intracellular organelles.[19] Scientific reports have claimed the presence of H_2S as gasotransmitter due to its stimulatory and inhibitory effects on nerve cells, cardiovascular system, endocrine system.[20] Additionally, its role in cardioprotection from ischemic reperfusion injury and dialation of blood vessels have highlighted the protective nature. The physiological effects of H_2S are exerted at a very low concentration of 10-100 μM.[21]

In aqueous solution, H_2S is weakly acidic and dissociates to form hydrosulphide anion (HS^-) at pK_{a1} 7.04. As such, at physiological pH of 7.4, approximately 81.5% of total H_2S exist as the HS^-anion. It is currently not known whether the biological effects of H_2S are mediated directly by H_2S itself or other derived species that will also exist at pH 7.4 (such as S^{2-} or HS^-).[22]

In mammalian cells, endogenous H_2S is produced via two pathways cysteine oxidation pathway and reverse transsulfuration pathway in the presence of three enzymes: cystathionine beta-synthase (CBS), cystathionine gamma-lyase (CSE) and 3-mercaptosulfurtransferase (3-MST).\

Cystathionine acts as an important intermediate in many sulfur containing amino acids in the presence of CBS. Further in the presence of CSE, L-cystathionine reacts with cysteine to form H_2S, L-cysteine, pyruvate, and ammonia. Cysteine reacts with α-ketoglutarate in the presence of cysteine

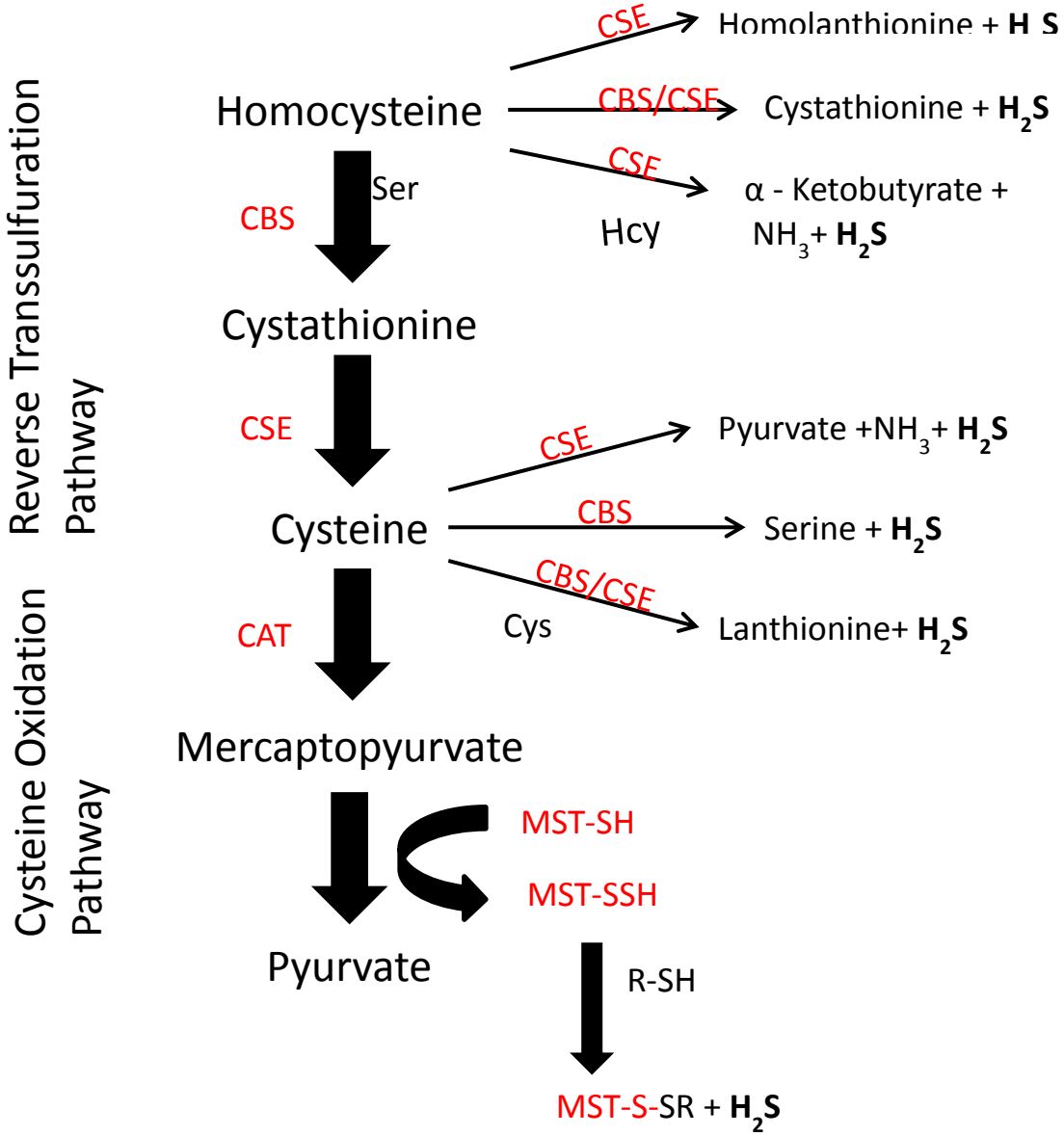

Figure 1.3 Various H_2S generating reactions catalyzed by enzymes in the reverse transsulfuration pathway (CBS and CGL) and the cysteine catabolic pathway (CAT/AAT and MST).[23]

aminotransferase (CAT) to yield 3-MST which acts as the substrate for cysteine catabolic pathway. 3-MST breaks down 3-mercaptopyurvate into pyruvate and persulfide (Fig. 1.3). H_2S is released in the presence of a reductant such as thioredoxin substrate and NADPH.[24,25] To understand the working mechanism and physiological activity in very low molecular concentrations, the detection and quantification of small gaseous molecules especially NO_2 and H_2S in biological system is a major hurdle to overcome.

1.2 Detection of small gaseous molecules

1.2.1 Traditional methods of detection and quantification

Detection and quantification of molecules have always been challenging domain of science, where precision and selectivity plays a pivotal role. In the case of gaseous molecules, methylene blue assay based detection of H_2S or Greiss method based detection of NO_2^- and NO_3^- were the roots for spectrophotometric based detection.[26,27] On the other hand, electrode based detection such as ion selective electrodes was also used profusely for detection of gaseous molecules. In the biological samples or cellular level detection, fluorescent probe based spectrometry and chromatography followed by protein based probes are the order of the day.[28] Several probes for detection of small gaseous molecules have been commercialized and available for rapid and sensitive detection such as diaminofluorescein based fluorescent probes for NO detection and WSP-1 probe for selective visualization of H_2S. In specific, the detection of intracellular molecules using fluorescent probes coupled with high quality imaging have provided more sensitive and selective visualization.[29,30]

1.2.2 Fluorescent probes for visualization of NO and its oxidation products

The physiological and pathological effects of NO and its reaction products have necessitated the development of sensitive and selective quantification techniques. Fluorescent probe based bio-imaging would give insights on the *in vivo* changes. A fluorescent probe compatible for biological imaging is ideally to be water soluble, membrane permeable, non-autofluorescing and rapidly reacting with analyte at low concentrations by turning on the fluorescence signal.[31] The fluorescent probe based detection of NO was classified into

organic-based and metal-based sensors. The former class represents compounds utilize complex benzene-ring structures as fluorophore to quench the fluorescence until reaction with NO. Whereas the latter class utilizes the reaction of NO at the metal site or a site near the metal binding.

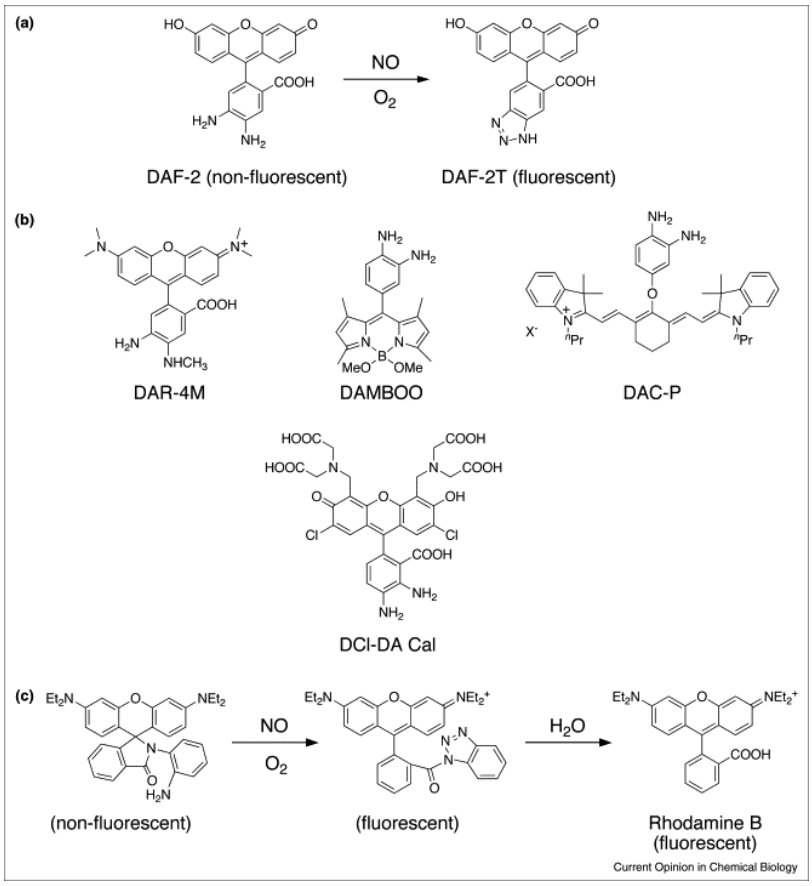

Figure 1.4 (a) Reaction mechanism of fluorescent probe containing diaminofluorescein fluorophore, (b) Fluorescent probes containing rhodamine, BODIPY, cyanine and calcein fluorophores, (c) Sensing mechanism of spirolactam ring opening by reaction with oxidized NO.[32]

Diaminofluorescein derivatives were the first class of compounds used for NO sensor, which utilized the reactivity aromatic vicinal diamines with NO in the presence of dioxygen to alter the photo induced electron (PeT) transfer restoring the fluorecnece.[32] Fluorescein based probes had the limitation of pH and photobleaching and gave way for rhodamine-based, BODIPY (Boron-dipyrene) (Fig.1.4) based sensors, and latest is cyanine based near-infrared

probes well suited for live tissue imaging.[33, 34]

Increased cellular retention of fluorescent probes were designed for monitoring small changes in biological levels of NO. The calcein based fluorescent probe DCl-DA, had increased cellular retention in HeLa and BAEC cells due to its imidodiacetate groups.[35] Rhodamine B spirolactam has a closed ring conformation abolishing the aromaticity which is directly related to fluorescent emission. Oxidized NO (believed to be N_2O_3) reacts with the adjacent diamines to produce the ring-opened, and therefore fluorescent, rhodamine B acylbenzotriazole, which quickly decomposes to yield rhodamine B.[36] The organic NO probes from non-reversible bonds and does not react directly with NO which led to advent metal based fluorescent probes working on the displacement of metal from the ligand leading to fluorescence. The Cu(II)-FL complex strategy of sensing has been well used in detection of NO due to its non-reactivity with other radicals such as NO_2^-, NO_3^-, H_2O_2, HNO, $ONOO^-$, $O_2^{\bullet-}$, and ^-OCl. The reaction mechanism consists of Cu(II) reduction to Cu(I) and the ligand is *N*-nitrosated to produce the fluorescent species, FL-NO, which dissociates from the metal center.[37] A similar sensor was reported with the fluorophore 4-methoxy-2-(1*H*-naphtho[2,3-*d*]imidazol-2-yl)phenol (MNIP) quenches the fluorescence and NO assisted reduction Cu(II) to Cu(I) produce fluorescence. Both the CuFl and MNIP-Cu based fluorescent probes were ideal for biological imaging of NO in different samples and were extended to animal imaging.[38]

Peorxynitrite is an oxidation product of NO and a strong RNS capable of nitrating amine directly bound to DNA. Several sensors with quenched fluorescent dye have been reported for the detection of peroxynitrite, which

forms highly fluorescent oxidized species. 2,7-dichlorodihydrofluorescein diacetate ($DCFH_2$) and dihydrorhodamine 123 (RhH_2) have reduced xanthene rings that are oxidized in the presence of peroxynitrite to form fully conjugated, and fluorescent, dichlorofluorescein (DCF) and rhodamine 123 (Rh), respectively.[39] However, the oxidation can be accomplished by any radical OH, $^{\cdot}NO_2$, $^{\cdot}CO_3^{-\cdot}$, Fe(II), Fe(III)/ascorbate, Fe(III)/EDTA, cytochrome c, HOCl, and H_2O_2 in the presence of peroxidases.[40] The selectivity of the probes fluorescein-based and rhodamine-based probes were improved by addition of ketone to phenolic oxygen of xanthene ring, thereby selective reaction with ketone which releases the fluorophore.[41] Recently, a BODIPY based fluorescent probe, HKGreen-2, was prepared that does not require cleavage of the oxidized phenyl group, whereas the difference in energy will abolish the PeT to restore fluorescence. The HKGreen-2 was applied in the cellular system to detect the iNOS-induced $ONOO^-$ formation in live cells.[42]

1.2.3 Detection and live cell monitoring of H_2S using florescent sensors

In the past decade, H_2S has deemed its status as a gasotransmitter and wide range of research has been carried out on its physiological role, redox properties, signaling cascades, anti-tumor effects and tissue protective measures. The detection of H_2S in biological system is a challenging task given its short half-life, easily diffusible nature and low molecular concentration.[92] Most of the fluorescent probes which showed greater selectivity and sensitivity towards H_2S in chemical system could not provide the same results in biological system due to the interference with other thiol based molecules. To overcome these challenges, several reports adopted different molecular frameworks. The H_2S sensitive fluorescent probes are

grouped into three classes based on the reaction mechanism. H_2S-based azide reduction to form fluorescent amine were the basis for earlier reports, which utilized rhodamine fluorophore for H_2S turn-on fluorescence in solution and biological systems. It exhibited greater selectivity over other biothiols and this

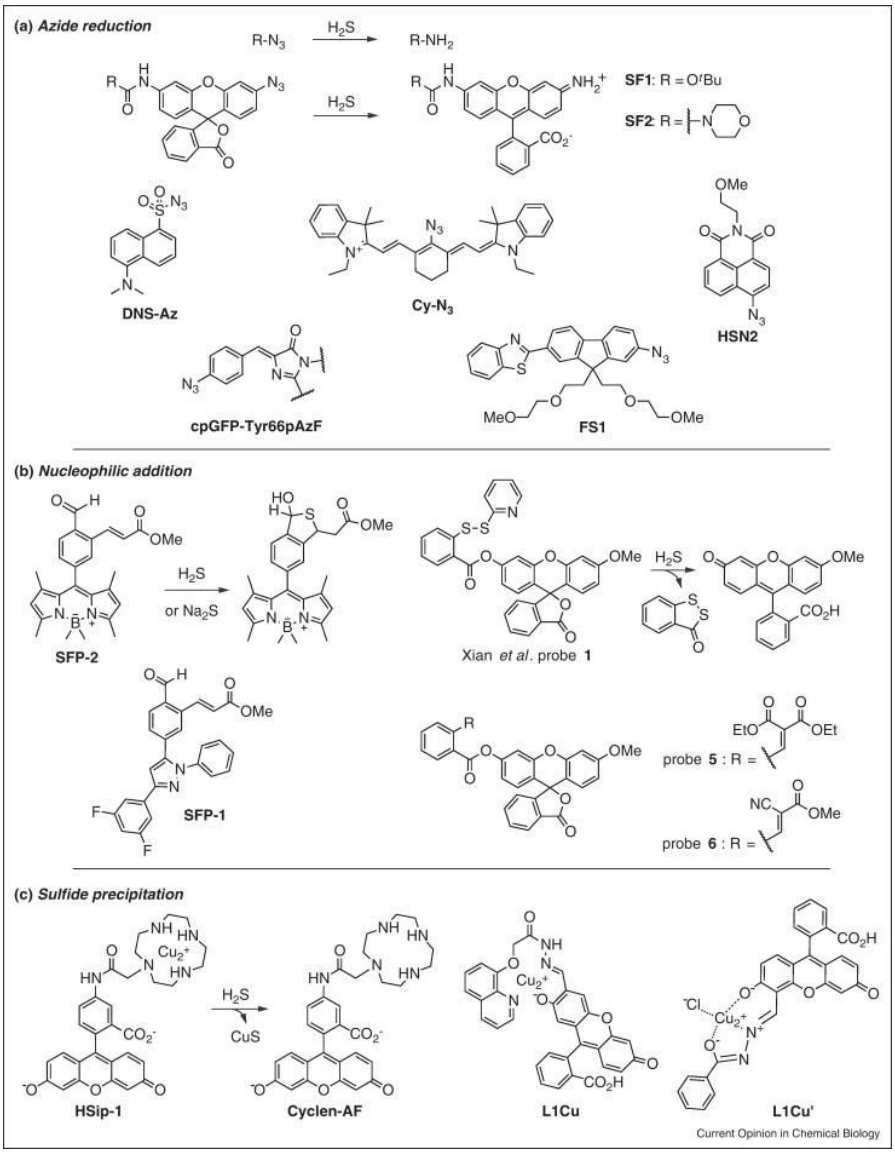

Figure 1.5 Selected molecular probes for the detection of hydrogen sulfide. (a) The H_2S-mediated reduction of azides to amines has been applied to rhodamine (SF1 and SF2), dansyl (DNS-Az), cyanine (Cy-N_3), 8-naphthalimide (HSN2), protein (cpGFP-Tyr66pAzF);(b) Reaction mechanism of fluorescent probes SFP-1 and SFP-2 with the addition of H_2S forms fluorescent dye. Whereas nucleophilic addition of H_2S to (Xian *et al.*) probe 1 results in intramolecular cyclization generating benzodithiolone with the release of 3-*O*-methoxyfluorescein. Two other variants of probe 1 with different Michael acceptors benzylidienemalonate and cyanoacrylate; (c) Reaction mechanism of H_2S with $Cu^{(II)}$ in HSip-1 and conversion of L1Cu and L1Cu` to form fluorescing moieties.[43]

led to the biological application of the fluorescent probes.[44] A simpler probe based on dansyl group was reported wherein addition of H_2S reduces sulfonyl azide into sulfonyl amide with strong fluorescent enhancement. This probe showed high sensitivity at lower working concentrations and detected H_2S bovine serum and blood samples.[45] Heptamethine-cyanine was the first among intramolecular charge transfer (ICT), which utilized H_2S mediated reduction of electron-withdrawing azido group into an electron-donor amino group associated with increase in fluorescence. In the same period of time, hydrosulfide naphthalimide-2 (HSN2) was reported with a masked fluorogenic amine group as azido or nitro group, which is tuned-on in the presence of H_2S. Both probes utilized different fluorophores whereas the reaction moiety was azide group. It showed greater sensitivity in intracellular detection without any interference from other biological analytes.[46,47] In recent times, genetically encoded H_2S probe was synthesized by substituting p-azidophenylalanine (pAzF) for Tyr66 in circularly permuted green fluorescent protein (cpGFP). The azide reduction mechanism was applied in cpGFP-Tyr66pAzF facilitating the formation of mature chromophore and eliciting a fluorescent turn-on response.[48] Lastly, a two-photon probe derived from 7-(benzo[d]thiazol-2-yl)-9,9-(2-methoxyethoxy)ethyl-9H-fluorene (BMF) as the reporter and azide moiety as the H_2S reaction site. The probe can detect intracellular sulfide in living cells with good signal-to-noise ratios in the presence of other biologically relevant analytes under physiological pH conditions. Further, the probe can be applied to detect H_2S in live cells and tissues at 90–190 μm depth by using two-photon microscopy.[49]

Nucleophilic addition of H_2S to the probe of interest leads to a cyclization

process generating a fluorescent molecule. H_2S biosensor based on 1,3,5-triaryl-2-pyrazoline and BODIPY as fluorophore, where aldehyde and α,β-unsaturated acrylate methyl ester groups (*ortho* to each other) produce dihydrobenzothiophene derivatives in the presence of H_2S (Fig. 1.5b). This aromatic framework aids in spontaneous reaction between aldehyde and free sulfide to form hemithioacetal intermediate with an exposed thiol. The exposed thiol group follows Michael's addition to the proximal acrylate group to yield trapped thioacetal with a photoinduced electron transfer in the aromatic system causing a change in the fluorescence. These fluorescent probes were suited for live-cell imaging as they exhibit significant fluorescence enhancement in response to Na_2S and H_2S in a high thiol background. The BODIPY based dye was further investigated in animal samples, wherein linear relationship between emission intensity and sulfide concentration was observed in biological bovine plasma systems.[50,51] Another H_2S fluorescent biosensor based on methoxyfluorescein, which was masked by an ester group with adjacent disulfide bond. The Michael's addition of H_2S resulted in the initial generation of the S--SH group owing to the nucleophilic substitution reaction between the masked fluorescein and H_2S at the disulfide bond, which undergoes further cyclization to produce a fluorescent molecule (Fig. 1.5b). This probe demonstrated greater selectivity for H_2S over other biological thiols *in vitro*, because displacement of the thiopyridine by a substituted thiol results in a mixed disulfide which does not undergo cyclization. Two additional probes that feature benzylidienemalonate or cyanoacrylate moieties as sites for Michael addition.[52,53]

This approach utilizes the displacement of Cu(II) from the fluorophore's

environment to produce fluorescence turn-on changes *via* H_2S mediated precipitation of CuS from Cu(II) Initially, the presence of paramagnetic Cu(II) centre quenches the emission of the fluorophore. However, H_2S mediated precipitation of CuS introduces fluorescence turn-on activity. H_2S imaging probe 1 (HSip-1), which consists of fluorescein with a cyclen macrocycle bound to Cu(II) reacts with sulfide and release the cyclen, which shows enhanced fluorescence. HSip-1 was applicable at lower concentrations *in-vitro,* however, the application in cellular system had membrane permeability problems.[54] The L1 sulfide probe consisted of fluorescein with 8-hydroxyquinoline suited for paramagnetic copper binding. Coordination of copper to L1 quenches fluorescence and produces a spectral shift when the probe is converted to the L1Cu metal complex. The addition of sulfide anions triggers precipitation of CuS and regeneration of L1 with fluorescent enhancement and change in colour from pink to yellow at micromolar concentrations.[55,56] The selectivity studies play an important role in Cu^{2+} precipitation based probes as Cu^{2+} complexes may react with RNS, ROS and sulfur containing molecules such as cysteine, glutathione. [54]

1.3 Fluorescent probing and image based analysis

The fluorescent probe based detection of gaseous molecules h has several criteria to be satisfied: (1) Fluorescent probes should react with molecule of interest to yield the corresponding fluorescent products without forming by products at room temperature at atmospheric pressure under physiological pH conditions in an aqueous solution and not with other interacting molecules; (2) The reaction should be specific to the molecule of interest; (3) Both of the probes and the products should be stable, especially to light, because laser

microscopy is used for bioimaging; (4) The difference in fluorescence properties should be easily distinguishable in the presence and absence of molecule of interest; (5) Visible light is desirable for excitation to diminish autofluorescence and photodamage to living systems; (6) The probes should be membrane-permeable so that they can enter living cells for bioimaging. In addition, ROS such as $O2^{\bullet-}$, $^{\bullet}OH$, etc., are often generated in cellular environment. Thus, a practical detection method is required which is satisfactory for studies in living cells in terms of distinguishability of molecule of interest from other interacting molecules (ROS and RNS).[43]

The fluorescent probes based detection of small gaseous molecules has been progressing at a good pace due to the advent of high precision instruments and application oriented research. The fluorescent probe has opened up several applications in biological domain such as live cell monitoring, intracellular 3-D analysis, time and location based scanning and *in vivo* animal imaging. All these methods are qualitative based analysis, which addresses the cell morphology, detection and localization.[57,58] While a quantification of fluorescent change inside the cell is still relied on microplate reader, spectrophotometer and chromatography based techniques which involves sample damage and interaction of cellular constituents. It is to be noted that combined qualitative and quantitative analysis in biological system without damaging the sample would be a progressive tool in understanding the cellular uptake level.[59,60]

1.4 Dissertation overview

This thesis describes the *in vitro* application of fluorescent probes in cellular system for selective and sensitive detection of nitrogen dioxide (NO_2) and

hydrogen sulfide (H_2S). The confocal fluorescent imaging followed by quantitative fluorescent intensity analysis was applied to determine the localization, intracellular concentration and interactions

Chapter 2 constitutes of Ni bisdithiocarbamate complexes based fluorescent probes for selective detection of NO_2. Sulforhodamine B fluorophore containing Ni complex was applied in selective detection of exogenous NO_2 in RAW 264.7 cells. 3-D imaging revealed the localization and site of NO_2 generation inside the cells. Fluorescent intensity quantification values were plotted to obtain an intracellular dose response curve. It also emphasizes on a cationic liposome based delivery of hydrophobic probes. The fluorescent probe was further optimized with a Rhodamine B fluorophore to aid in endogenous NO_2 generation. LPS induced endogenous NO_2 was monitored in live cell to exhibit intracellular sensitivity and selectivity was analyzed in the presence of L-NAME, which inhibits the LPS stimulated NO_2 production. Fluorescent intensity quantification explained the direct relationship between LPS stimulation time and inctracellular NO_2 levels.

Chapter 3 outlines the BODIPY based Cu(II)-cyclen complex fluorescent probe for intracellular localization of H_2S supplied by Na_2S and NaHS. The fluorescent probe showed intracellular detection limit of 25 μM Na_2S and no interaction with other thiol containing compounds such as cysteine and glutathione. A unique image based quantification approach was applied in quantifying the fluorescent intensity from individual cells and dose response was plotted in reference to concentration. The fluorescent probe was further applied in understanding the H_2S release profiles of natural polysulfides and synthetic slow H_2S releasing compounds in MCF-7 cells. The sensitivity of

probe towards low concentration H_2S lead to the detection of endogenously generated H_2S via overexpression of CSE gene in HEK 293 cells.

In Chapter 4, combination of NO_2 and H_2S sensitive probe was successfully delivered into RAW 264.7 cells using DOTAP liposome. Simultaneous monitoring of NO_2 and H_2S and possible interactions were studied. The endogenous NO_2 levels were monitored with relevance to concentration time based approach.

Chapter 2. Detection of Exogenous and Endogenous Nitrogen Dioxide by Nickel (II) Dithiocarbamate Complex Based Fluorescent Probes

2.1 Introduction

Fluorescent probes sensitive for NO_2 detection without interacting with other RNS would be the choice for selective detection NO_2. It is reported that that Ni bisdithiocarbamate complexes, $Ni(RNCS_2)_2$, react rapidly with NO_2 to yield the fluorescent oxidative dimerized ligand, $(RNCS_2)_2$ where R is the fluorophore.[64] Dithiocarbamate is a bidentate ligand that can easily form coordination compounds with various transition metals.[61,62] Nickel acts as an efficient fluorescence quencher through electron transfer process. The ortho isomer showed greater fluorescence increase upon reaction with NO_2, leading to oxidation and decomplexation of the dithiocarbamate ligand from Ni(II).[63] This probe was successfully applied in cellular model to determine the selectivity and sensitivity. Further due to low yield and poor solubility in organic solvents, an improved version was needed for endogenous NO_2 detection. To continue with Ni based dithiocarbamate complex, which had selective reactivity towards NO_2 allowed us to work on the fluorophore. The rhodamine B derived bis(dithiocarbamato)Ni(II) complexes showed best response factor towards NO_2 had an improved organic solvent solubility and greater fluorescence.

The two probes displayed high selectivity towards NO_2 dissolved in aqueous buffer solutions and greater selectivity in a pool of other biomolecules and radicals.[76] The probe satisfied all the basic requisite of fluorescent NO_2 biosensor except the hydrophobic nature prohibiting it from transfer across membranes. It required a proper mechanism in order to facilitate its delivery through the lipid bilayer membrane.

Cationic liposomes are amphiphilic molecules consisting of cationic polar

head, a non-polar tail and a linker molecule. From the late 20th century, cationic liposomes are extensively used in gene therapy over the viral vector methods, due to high delivery efficiency, non-limiting to DNA size and does not initiate any immunogenic or inflammatory response.[65] The working mechanism behind cationic liposome was the formation of lipid-DNA complex or lipoplex which transverses through the plasma membrane and forms an endosome. In the presence of cellular esterases, the endosome is broken with the release of DNA.[66]

The hydrophobic nature of the fluorescent probes necessitated a proper delivery mechanism into the cellular membrane. Cationic liposomes were found to be an apt candidate for the delivery of fluorescent probe, thereby to detect the physiological changes. DOTAP (1,2-dioleoyloxy-3-trimethylammonium propane) is a well-known transfection lipid consisting of a monocationic trimethylammonium (head), glycerol (linker) and two unsaturated hydrocarbon chains, derived of oleic acid (tail) was chosen for the delivery of fluorescent probe. [67]

As a dominant component in the NOX family, nitrogen dioxide (NO_2) is a toxic air pollutant mainly generated by the combustion. The effects of NO_2 to human depend on the level and duration of exposure, ranging from chest pain to lung disease, even death.[68] The biological consequences of low levels of endogenously produced NO_2 have started to be considered only recently.[69] The neutral radical is likely to accumulate to a higher concentration in less polar environments such as cell membranes and hydrophobic protein domains. In physiological system, NO_2 undergoes a variety of reactions including recombination with other radical species, addition to double bonds, electron

transfer and hydrogen atom abstraction. It can initiate lipid peroxidation and oxidize amino acids, particularly cysteine, tryptophan and tyrosine, generating nitrated lipids and proteins, which have been extensively used as markers of nitric oxide-derived species in injured tissues and cells from diverse pathologies.[70]

Diethyl NONOate (DEANO) is potent NO donor capable of releasing NO in a clean, first-order reaction with a half-life of 2.1 minutes at 37°C and pH 7.4. NONOates are secondary amines containing NO adducts and also known as diazeniumdiolates. Due to its lack of stability, DEANO is always maintained in -20°C and higher pH solution for dissolving in order not to lose NO donating ability.[71] DEANO showed good results in chemical system as the oxygen rich environment converted the released NO into NO_2, sensitive to the fluorescent probe[76] The releasing profile in chemical system and fast releasing nature of DEANO allowed us to carry forward to exogenous NO_2 imaging in RAW 264. 7 cells.

On the other hand, endogenous NO_2 production in RAW 264.7 cells was induced by lipopolysaccharides (LPS). Inducible NOS (iNOS) is expressed in macrophages during inflammation through the stimulation of interleukins and endotoxins. The macrophagic origin of RAW 264.7 cells and LPS as endotoxin stimulant was utilized in endogenous NO production, thereby generated NO would be rapidly autoxidized into NO_2 within the membrane due to the aerated media. The NO_2 levels are usually low during physiological conditions and increases rapidly during pathophysiological conditions.[72] The iNOS converts the arginine transported across the cell membrane into nitric oxide and citrulline. The methyl ester substituted nitro-arginine (L-NAME) is

a structural analogue of L-arginine, which reduces the transport of arginine into the cells through cationic ion transporter. The unavailability of arginine substrate ceases the NO production through iNOS pathway.[73]

2.2 Materials and Methods

2.2.1 Materials and Instruments

All experiments were performed with analytical grade reagents. Otherwise stated, all chemicals were purchased from Sigma-Aldrich Chemical Company (St Louis, MO) and used without further purification. Ultrapure water (18.2 MΩ˙cm) was used from a Millipore water purification system. NO_2 selective fluorescent probe, a sulforhodamine B containing nickel(II) dithiocarbamate complex was prepared according to this reported method.[76] Rhodamine B derived nickel(II) dithiocarbamate complex was gifted from Yan Yan. Fluorescence measurements were carried out using a Synergy HT microplate fluorescence reader from Bio-Tek Instruments Inc., (Winooski, Vermont), installed with KC4 software and Tecan Ultra 384 Micro plate reader. Fluorescence spectra were obtained on PerkinElmer LS55 fluorometer with slit width at 10 nm for both excitation and emission. Fluorescence spectra were obtained on PerkinElmer LS55 with slit width at 10 nm for both excitation and emission except fluorescence quantum yield measurement. Cellular 3D and 2D images were captured using Olympus IX 81, Fluroview FV1000 confocal microscopy equipped with a 60X water lens. Further the images were processed using IMARIS 3.0 (BITPLANE AG) and imageJ software.

2.2.2 Cell culture

The Mouse leukaemic macrophage cells (RAW 264.7) from the American Type Culture Collection (ATCC, Manassas, VA, USA) were

cultured in DMEM (Dulbecco's modified Eagle's medium, GIBCO Grand Island, NY, USA) with 10% fetal bovine serum (FBS, Hyclone), 1% glutamine, 100 U/mL streptomycin and 100 μg/mL penicillin. The cells were maintained at 37 ^{o}C in a 5% CO_2 humidified environment. Eppendorf centrifuge (5804R) equipped with a F-34-6-38 rotor was utilised for passaging and supernatant separation.

2.2.3 Optimization of probe 1: DOTAP mixing ratio

Piperazine containing nickel(II) dithiocarbamate complex was used in optimizing probe: DOTAP concentration for proper delivery into the cells. The RAW 264.7 cells were seeded at $2x10^4$ cells per well in 96 well plate and incubated overnight. The cells were washed and transferred to fresh DMEM containing piperazine based nickel(II) dithiocarbamate complex mixed with DOTAP liposome (1:50,1:100,1:20). During the incubation time, intermittent checking of morphology and overall cell count was carried out to check for deleterious effects. The 96-well plates were incubated at 1h, 2 h, 4 h and 8h and then fluorescent intensity was measured at excitation 540 nm and emission 560 nm using Synergy HT microplate fluorescence reader from Bio-Tek Instruments Inc.

2.2.4 Encapsulation of probe 1 in DOTAP liposome

DOTAP (28 μL, 25 mg/ml in chloroform) and probe 1 (67 μL, 1 mg/mL or 645 μM in dichloromethane) were taken in a glass vial. The solvent was evaporated using a stream of argon. The resulting lipid film was further dried under vacuum for 20 min to remove the traces of chloroform. The lipid film was hydrated with 1 ml of de-ionized water and sonicated for 5 min to give clear solution of liposome with DOTAP and probe 1 concentrations at 1.0

mM and of 50 μM respectively.[93] The probe- DOTAP mixture (1:20) was protected from light and stored in ice. It was further diluted to 5 μM and 100 μM using DMEM to obtain the working concentration.

2.2.5 Cytotoxicity profiling of DOTAP liposome and fluorescent probes

Cytotoxicities of 1,2-dioleoyl-3-trimethylammonium-propane chloride salt (DOTAP, 25 mg/ml) in chloroform, sulforhodamine-B containing nickel(II) dithiocarbamate complex (probe 1), rhodamine-B containing nickel(II) dithiocarbamate complex (probe 2) was measured using CytoTOX96 non-radioactive cytotoxicity assay kit (Promega, Madison, WI, USA). Raw 264.7 cells were seeded at 2 x 10^4 cells/well in a 96-well flat bottom plate (Corning Glass Works, Corning, NY, USA) and incubated for overnight in DMEM (Dulbecco's Modified Eagle Medium) with 10% fetal bovine serum at 37 ^{o}C in 5% CO_2 humidified environment.

Probe 1 was weighed at 0.1 mg and dissolved in equal volume of dichloromethane - DMSO (67 μl, 1.0 mg/ml). Similarly, probe 2 was weighed at 0.1 mg and dissolved in equal volume of dichloromethane - DMSO (40.2 μL, 1.0 mg/ml). Both the solutions were further diluted to the working concentration (1- 50μM). DOTAP (28 μl, 25 mg/ml in chloroform) taken in a vial was evaporated using a stream of argon. The resulting lipid film was further dried under vacuum for 20 min to remove the traces of chloroform. The lipid film was hydrated with 1ml of de-ionized water and sonicated for 5 min to give clear solution of DOTAP liposome 1.0 mM. The working concentration (12.5 μM-400 μM) was obtained by dilution with DMEM and added to the culture wells.

Cells cultured in DMEM without any treatment served as low control. The Culture plate was incubated for 4 h at 37 ^{o}C and 5% CO_2 humidified environment. The spontaneous lactate dehydrogenase (LDH) release was measured by performing the LDH assay as prescribed by the manufacturer on the media supernatant. Triton X-100 was added to the wells to determine maximum LDH release in individual wells. The 96-well plate was centrifuged at 1000 x g for 10 min to separate the cell debris. The absorbance was measured at 490 nm using Tecan Ultra 384 Micro plate reader. The cytotoxicity was expressed as the percentage between the result of the Spontaneous LDH and that of the maximum LDH from the same time.

2.2.6 Confocal Imaging of exogenous NO_2 release in the cell

The RAW 264.7 cells cultured in 10mm cell culture plates were centrifuged and the pellet was re-dissolved in 1ml fresh DMEM for transfer to culture plates. The cell suspension (10^6/ml) was seeded on a chambered coverglass (Lab-Tek chambered #1.0 Borosilicate Coverglass System). After 24 h, the media was discarded and cells were washed with phosphate buffered saline (PBS) thrice. The probe- DOTAP mixture (1:20) was diluted to 5 μM using DMEM and added to each well. After 4 h, the medium was discarded and cells were washed with PBS to remove excess probe-DOTAP in the well. The intracellular localization of probe-DOTAP mixture in single cell was investigated by a sequential z-step scanning using confocal microscopy (Olympus IX 81, Fluroview FV1000) equipped with a 60X water lens. Probe-DOTAP mixture was excited with a 540 nm Ar laser, and the fluorescent images were collected using filter sets more than 560 nm. Images were processed in IMARIS 3.0 (BITPLANE AG) software.

The cells were then transferred to fresh media with DEANO (0, 0.2, 0.5 and 1mM) at room temperature. Central sections of cells were chosen to observe the fluorescent changes of probe-DOTAP mixture. The images were recorded with the same optical parameters of confocal microscopy at a time interval of 10 min. The fluorescence intensity quantification is calculated using Image J software.

2.2.7 Detection of endogenous NO_2 by Rhodamine B based fluorescent probe

The sulforhodamine B based nickel(II) bisdithiocarbamate complex fluorescent probe showed selectivity and sensitivity towards exogenous NO_2 released by DEANO. To utilize the probe for more sensitive in-vitro applications and detection of endogenous NO_2 released inside the cells, Rhodamine B fluorophore was utilized. The improved version of the probe was more suited for the endogenous detection due to the lower probe concentration, increased solubility in organic solvents.

DOTAP (28 μL, 25 mg/mL in chloroform) and probe 2 (40.2 μL, 1 mg/mL or 645 μM in dichloromethane) were taken in a glass vial. The solvent was evaporated using a stream of argon. The resulting lipid film was further dried under vacuum for 20 min to remove the traces of chloroform. The lipid film was hydrated with 1mL of de-ionized water and sonicated for 5 min to give clear solution of liposome with DOTAP and probe 1 concentrations at 1.0 mM and of 30 μM respectively. The probe- DOTAP mixture was protected from light and stored in ice. It was further diluted to 3 μM and 100 μM using DMEM to obtain the working concentration.

The Intracellular NO_2 was induced by lipopolysaccharides (LPS) (Sigma,

USA) through iNOS pathway. RAW 264.7 cells were cultured in chambered cover glass for 12 h were washed with PBS and stimulated with LPS (2 μg/ml) in DMEM for 8, 12 and 16 h respectively. Non-stimulated cells and cells treated with L-NAME (L-NG-Nitroarginine methyl ester) (Sigma, USA) for 2 h prior to 16 h LPS stimulation served as control and negative control respectively. After stimulation the cells were bathed with PBS thrice and treated with fresh DMEM containing probe-DOTAP (3 μM). The excess probe-DOTAP mixture was removed by washing with PBS after 2 h and fresh media was added. The intracellular localization of probe-DOTAP mixture in cells were investigated by a sequential z-step scanning using confocal microscopy (Olympus IX 81, Fluroview FV1000) equipped with a 60X water lens. Probe-DOTAP mixture was excited with a 540 nm Ar laser, and the fluorescent images were collected using filter sets more than 560 nm.

The exogenous NO_2 release in RAW 264.7 was also analyzed to compare with the LPS-induced endogenous NO_2. Cells cultured in chambered coverglass were washed with PBS and fresh DMEM with and/or without probe-DOTAP (3 μM) was added. After incubation for 2 h, the cells were washed with PBS thrice and DEANO (1mM) in DMEM was added. The 2D images were captured in different samples of the same treatment to improve the statistical data (n = 10) and to observe the fluorescent changes in probe-DOTAP with reference to non-DEANO treated control. The images were recorded with the same optical parameters of confocal microscopy at a time interval of 10 min. The fluorescence intensity quantification is calculated using ImageJ software.

2.3 Results and discussion

2.3.1 Probe 1: DOTAP ratio optimization

RAW 264.7 cells were treated with piperazine containing nickel(II) dithiocarbamate complex encapsulated in DOTAP liposome at different concentrations (1:100,1:50,1:20). The 96 well plates after the designated incubation time were analyzed for fluorescent intensity using a synergy HT microplate reader. The samples after 1h and 2 h incubation time did not show any change in fluorescent intensity for all three concentrations and morphology of the cell was maintained along with cell count. On the other hand, 8h treatment had marked change in morphology of the cell and cell count was diminished. The 4h treatment on 3 samples maintained the morphology and cell death was minimum compared to 8h. Fluorescent intensity quantified using microplate reader showed statsistcially significant increase in 1:20 concentration suggesting the minimum requirement of probe to be encapsulated within DOTAP liposome. (Figure2.1) The probe: DOTAP (1: 20) mixing ratio was further subjected LDH assay for an incubation time of 4h.

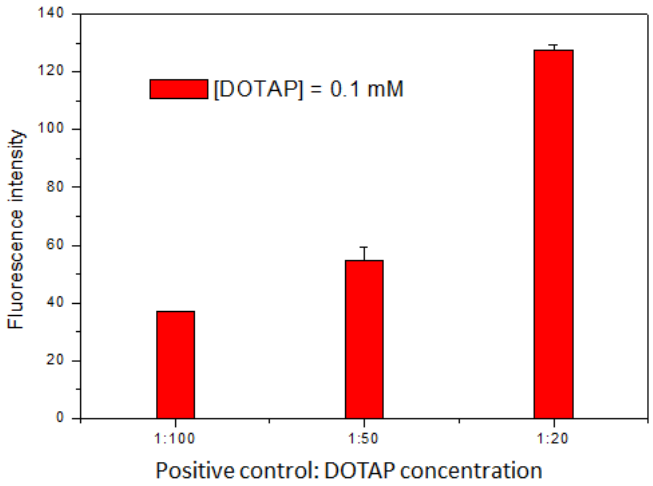

Figure 2.1 Fluorescent intensity quantification DOTAP-Probe mixing ratio (n = 5).

2.3.2 Cytotoxicity profile of DOTAP liposome and NO_2 sensitive probes

The *in vitro* cytotoxicity of DOTAP on RAW 264.7 cells was measured using CytoTOX96 non-radioactive cytotoxicity assay kit (Promega, Madison, WI, USA). The absorbance at 490 nm was measured for DOTAP

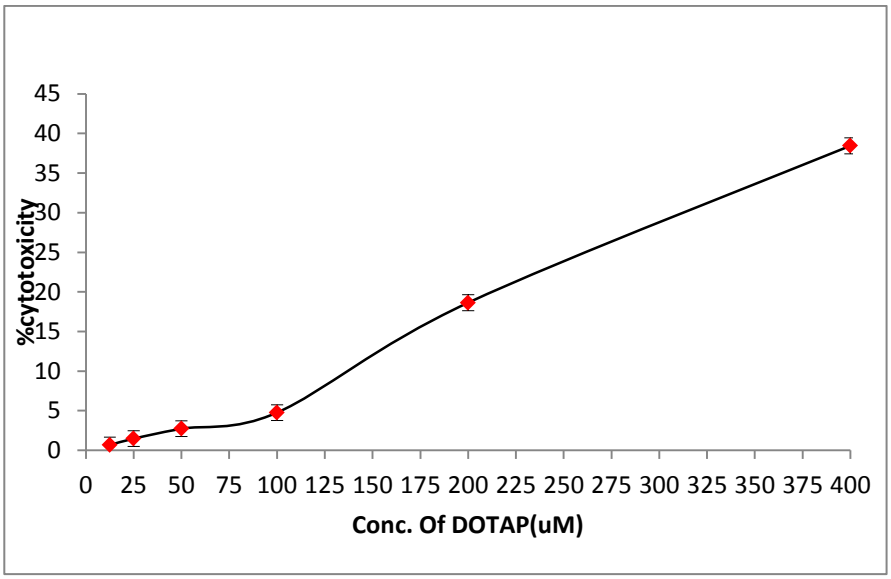

Figure 2.2 Cytotoxicity data for DOTAP at various concentrations after 4 h incubation with RAW 264.7 cells. The DOTAP at 100 μM adopted in the cell imaging experiment demonstrates negligible cytotoxicity (less than 5%).

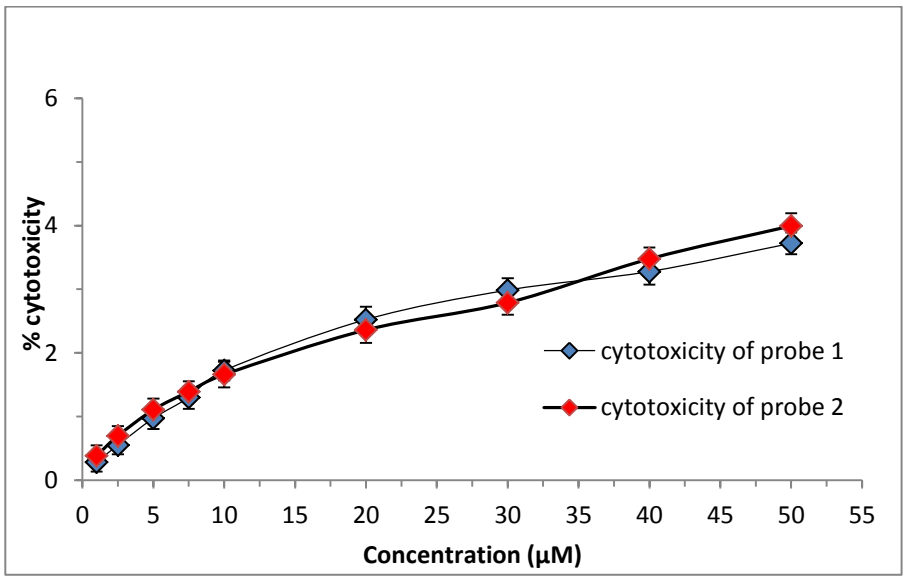

Figure 2.3 Cytotoxicity data for probe 1 and probe 2 at various concentrations after 4 h incubation with RAW 264.7 cells. The concentrations of probe at 5μM and 3 μM adopted in the cell imaging experiment demonstrates negligible cytotoxicity (less than 2%).

liposome at different concentrations (12.5 - 400 μM) and plotted into a cytotoxicity curve. The toxicity of DOTAP at the working concentration of 100 μM corresponded to minimum cell damage (less than 5%). (Figure2.2) The fluorescent probes were distributed at different concentrations (1- 50 μM) and LDH assay was performed. The cytotoxicity of the probes at their working concentration 5 μM and 3 μM in cellular imaging studies showed negligible toxicity (less than 2%). (Figure 2.3)

2.3.3 Localization of NO_2 in RAW 264.7 cells

The RAW 264.7 cells were mounted on the sample table of confocal microscopy and exogenous NO donor DEANO was added to the cells. The cellular environment abundant in oxygen converts the NO to NO_2 which is

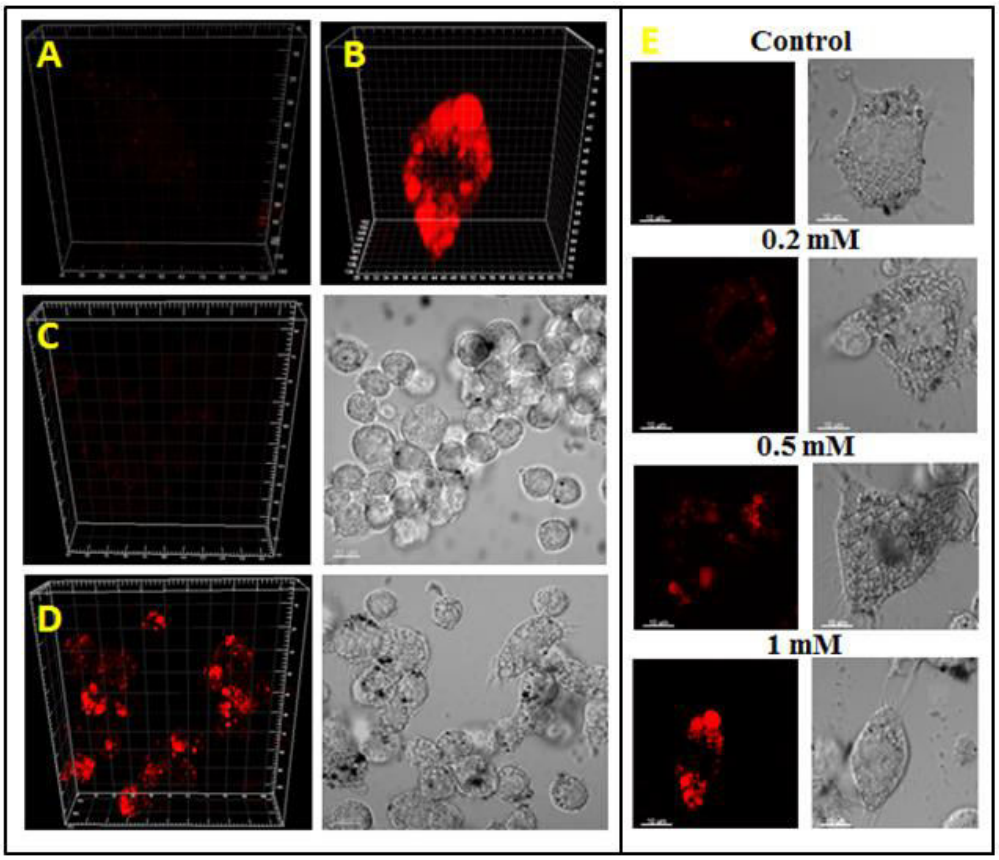

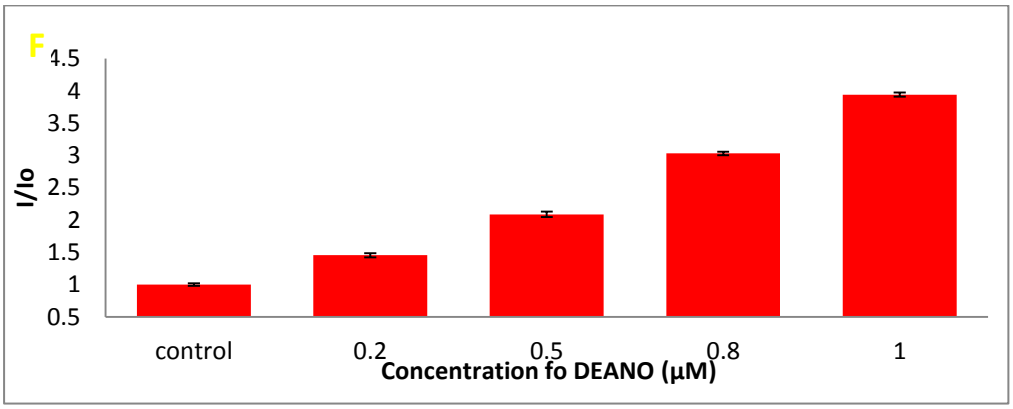

Figure 2.4 NO_2 turns on the fluorescence of RAW 264.7 cells stained with probe 1. (A) and (B) are 3D images of single cell not treated and treated with DEANO (1 mM) respectively.(C) and (D) are 3D images group of cells not treated and treated with DEANO (1 mM) respectively, together with their respective white field cell images.(E) Confocal fluorescent microscopes of cells treated with different concentrations of DEANO (0, 0.2, 0.5, 1 mM) and their respective white field cell images. (F) Fluorescence quantification of confocal images of RAW 264.7 cells stained with probe 1, with and without DEANO treatment (n = 5).

selectively localized by probe 1. The hydrophobic probe 1 encapsulated in DOTAP demonstrated good selectivity to NO_2 and a dose-response. The 3D sequential scanning was performed in order to unravel the localization of fluorescent probe in the cytoplasm, thereby giving a clear picture on the presence of NO_2.(Figure 2.4 B) The comparison with non-DEANO treated cells showed the marked increase in fluorescence.(Figure 2.4A and 2.4B) The uniform delivery of probe 1 into the cells by liposome mediated delivery and sensitivity of the probe was corroborated by the 3-D imaging of group of cells with and without DEANO treatment.(Figure 2.4C and 2.4D). The steady increase in fluorescent intensity with increase in DEANO concentration clearly showed the dose response relationship. (Figure 2.4E) The fluorescent intensity from the cells of different samples (0, 0.2, 0.5, 1 mM) were quantified using ImageJ software were utilized in plotting the intensity vs concentration curve (n = 5). The fluorescent intensity plot confirmed the significant increase in fluorescence with reference to DEANO treatment. (Figure 2.4F)

2.3.4 Detection of Exogenous and Endogenous NO_2 using probe 2

The sulforhodhamine-B based fluorescent probe (probe 1) showed good selectivity and sensitivity towards NO_2 in both chemical and biological system. To take the detection mechanism one step further for detection of endogenously produced NO_2 in RAW 264.7 cells, the fluorophore was replaced by rhodamine-B (probe 2) which showed higher change in fluorescent intensity and lesser probe concentration. Firstly, the probe was tested for detection of exogenous NO_2 using DEANO, which will be used

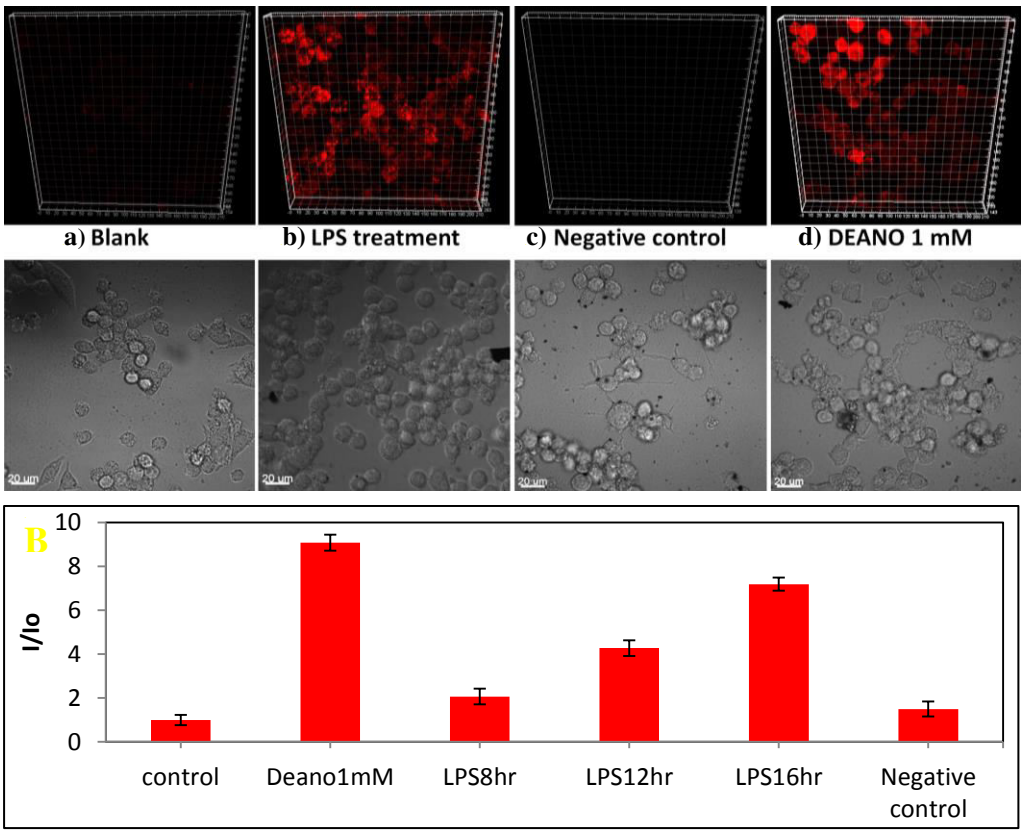

Figure 2.5 Detection of NO2 in RAW 264.7 cells by DOTAP-probe 2 mixture. The top images are 3D fluorescent images and bottom images are corresponding 2D DIC images. Cells a) treated with DOTAP-probe 2 mixture (3 µM) for 2 hours b) pre-stimulated with LPS (2 µg/ml) for 16 hours and treated with DOTAP-probe 2 mixture(3 µM) for 2 hours. c) sequentially treated with L-NAME(0.5mM) for 2 hours, LPS (2 µg/ml) for 16 hours and DOTAP-probe 2 mixture(3 µM) for 2 hours. d) incubated with DOTAP-probe2 mixture(3 µM) for 2 hours and DEANO (1mM) for 10 min. (B) Fluorescence quantification of confocal images of RAW 264.7 cells stained with the probe 2 for various treatments using imageJ software (n = 10).

for comparison with endogenous NO_2 production via iNOS (inducible Nitric

Oxide Synthase) pathway.

The macrophagic nature of RAW 264.7 cells were utilised for endogenous NO production via iNOS pathway. The iNOS pathway requires stimulants such as interleukin, interferons, endotoxin or tumor necrosis factor-α. LPS is a known endotoxin capable of stimulating the iNOS dependent NO production, which is rapidly autoxidized to NO_2 due to oxygen rich cellular environment.[71] The LPS induced production of NO_2 drastically increases the cellular concentration. Hence, to observe the fluorescent changes, a definite negative control wherein iNOS induces NO production is ceased. The methyl ester substituted nitro-arginine (L-NAME) is a structural analogue of L-arginine reduces the transport of arginine via cationic ion transporter into the cells. The unavailability of arginine substrate ceases the NO production via iNOS pathway.[72] RAW 264.7 cells were pretreated with LPS for 16 h were treated with DMEM containing probe 2 in DOTAP liposome for 2 h. The non-stimulated cells served as blank and cells simultaneously treated with L-NAME for 2 h followed by LPS stimulation for 16 h and probe 2 in DOTAP solution for 2 h served as negative control. (Figure 2.5A) The 3-D images of all DEANO and LPS treatment had marked increase in fluorescent intensity compared to the blank treatment. The marked increase in LPS treatment highlights the iNOS induced endogenous NO_2 generation. The negative control showed very negligible fluorescent intensity change suggesting the cease of NO_2 production. The fluorescent intensity of the samples was corroborated using intensity plot obtained among various treatments using image J software. (n = 10) (Figure 2.5B) The intensity plot confirms the increase in fluorescent intensity with reference to LPS stimulation. The different LPS stimulation

intervals were analysed for change in fluorescent intensity.

2.3.5 Analysis of time dependent increase in fluorescent intensity

The LPS stimulation was carried out at 3 different intervals 8 h, 12 h and 16 h in order to establish the relationship between LPS stimulation time and endogenous NO_2 generation. The fluorescent qualitative imaging coupled with intensity analysis supported with increase in fluorescent intensity is directly

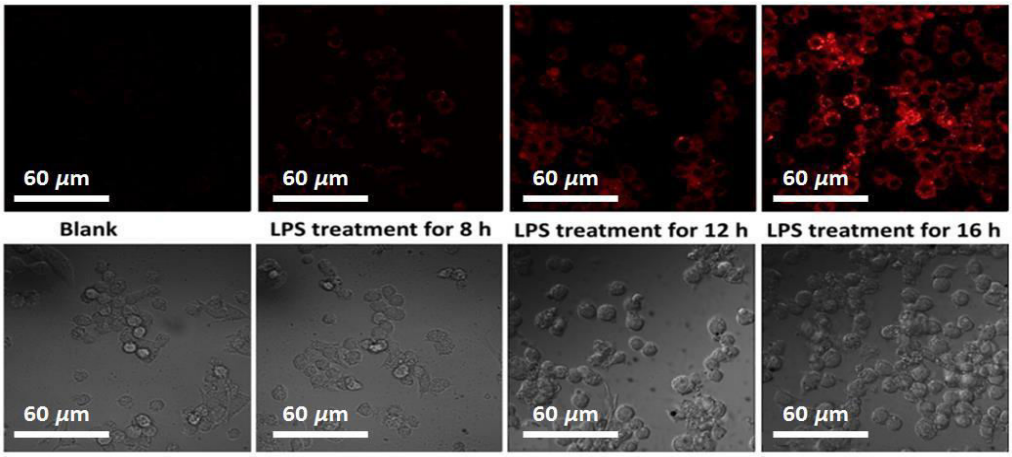

Figure 2.6 Endogenous NO_2 detection in RAW 264.7 cells by probe 2-DOTAP mixture. The upper panel is fluorescent images and the lower panel is corresponding bright-field images. The cells were treated with probe 2-DOTAP mixture (3 μM) for 2 h, then with LPS pre-stimulation (2 μg/ml) for 0, 8, 12 and 16 h, respectively.

related to the LPS stimulation time. The 2-D fluorescent images of 8 h, 12 h and 16 h had upward increase in fluorescent intensity when compared withnon- stimulated cells.(Figure 2.6) The intensity analysis using imageJ software was applied at different regions of same treatment to obtain a significant intensity value for the treatments. The values were plotted into an intensity plot and 16 h treatment had 7- fold increase in fluorescent intensity when compared to the blank. (Figure 2.5B) It is important that the fluorescent intensity based analysis should be taken further into the understanding the fate of NO inside cells. Several reports based on kinetic studies suggest the formation of N_2O_3 under aerial condition due to rapid coupling of NO_2 with

NO. It is the reversible nature of the reaction causing doubts on sensitivity of probe 2 on NO_2 alone or even N_2O_3. It will be relevant if N_2O_3 sensitive fluorescent biosensor can be simultaneously used with probe 2 in a macrophage cells.[74,75]

2.4 Conclusion

In summary, through systematic approach, We have illustrated that Ni(II) dithiocarbamate complex containing sulforhodamine and rhodamine-B fluorophores for sensitive and selective detection of exogenous and endogenous nitrogen dioxide generated in RAW 264.7 cells generated by DEANO and LPS over-stimulation respectively. The probe has great potential as a convenient tool for investigation of NO_2 biochemistry through fluorescent imaging. NO_2 is a potent RNS and can trigger lipid peroxidation and interact with DNA and proteins, which can lead to severe pathological effects, Hence the fluorescent probe acts as an important tool in screening of RNS scavenging compounds. Endogenous NO also interacts with other biomolecules and gasotransmitters inside the cell to exert various physiological effects which can be monitored using fluorescent imaging to aid in the understanding the mechanism of interaction and protective effects. Nitric oxide formation through in cells by nitric oxide synthase have been thoroughly studied and documented. Yet, the fate of formed NO in cellular systems is hard to pinpoint due to its rapid reaction with dioxygen and superoxide anion. The qualitative imaging coupled with quantitative fluorescent intensity measurement clearly highlights the production NO_2. However, the intracellular concentration of NO and NO_2, their inter-conversion, interaction with biological molecules is still to be addressed. The oxygen levels greatly influence the formation of NO

intermediates. The application of our fluorescent probe in combination with peroxynitrite specific fluorescent probe can aid in understanding the fate of NO inside the cells.

Chapter 3. Intracellular Localization of Exogenous and Endogenous Hydrogen sulfide by BODIPY Based Cu(II)-cyclen Complex Fluorescent Probe

3.1 Introduction

The detection of H_2S using fluorescent probe was carried out using BODIPY based Cu(II)-cyclen complex fluorescent probe. The probe contains Cu(II)-cyclen complex as a reaction center for H_2S and quencher of BODIPY (boron-dipyrromethene) derivative as fluorophore with λ_{ex} = 680 nm and λ_{em} = 765 nm respectively. The probe was designed as per the basic feature of fluorescent probe in order to detect the molecule of interest, H_2S. This emission range fluorescent probe in the near infra-red region distinguishes it from other reported fluorescent probes which are in the visible region(400-700nm).[77] This enables the probe for in vivo imaging without interfering the cellular matrix and living cells. The probe showed great selectivity towards H_2S and did not show any change in fluorescence with other biomolecules, radicals, and thiol containing compounds. The probe showed enhanced sensing potential towards H_2S at 80 nM in aqueous buffer solution.[77] These characteristics along with hydrophobic nature allowed us to utilize the same DOTAP liposome based delivery into the cells.

Na_2S and NaHS served as the exogenous H_2S donors. The difference between the two sulfide donors is based on purity. These two act as reference molecules and polysulfide screening can be interpreted in terms of NaHS equivalents. Poly sulfides are compounds formed by the unique ability of chain formation by sulfur atoms and the number of sulfur atoms determines the prefix of the molecule .

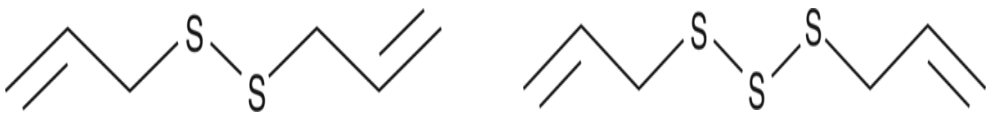

Figure 3.1 Molecular structure of diallyl disulfide and diallyl trisulfide.

The sulfur-sulfur bond plays a key role in maintaining the molecules in tertiary structures essential for their biological activity. Interconversion of sulfhydryl (−SH) groups play an important role in transport across cell membranes, immune process and blood clotting. The polysulfides are potential source of H_2S in the presence of reductant such as GSH. Diallyl disulfide and diallyl trisulfide were utilized for screening due to their previous reports on vasoactivity and cardioprotective characteristics.[78]

GYY 4137(morpholin-4-ium 4 methoxyphenyl(morpholino) phosphinodithioate) was recently reported for slow H_2S releasing nature. The compound showed anti-proliferative effect among various cancer cells without affecting the normal cell lines. Whereas, NaHS couldn't cease the proliferation in both the caner and normal cell lines. The H_2S releasing kinetics suggested

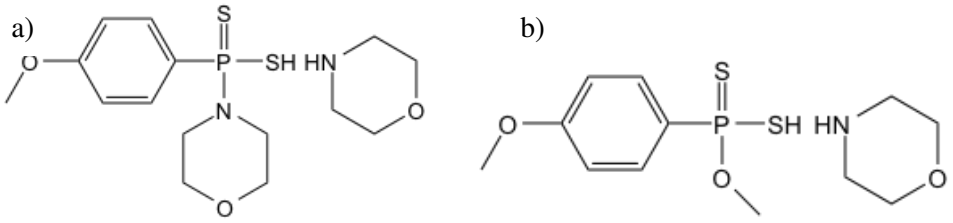

Figure 3.2 Molecular structure of a) GYY 4137 and b) FW 1010.[80]

a structural analogue FW 1010 also had extended release of H_2S across days. FW 1010 had enhanced concentration dependent killing across various cancer cell lines. The controlled and prolonged release of H_2S promotes its role in cancer therapeutics. The low and sustained release of H_2S by these two compounds served as the proper set up to test the sensitivity of the probe. [79,80]

Endogenous H_2S was generated in HEK 293 cells via siRNA-gene silencing and plasmid overexpression of cystathionine-γ-lyase (CSE). The crystal

structure analysis and site directed mutagenesis studies of human CSE lead to identification of amino acids in CSE that directly regulate the H_2S production. These specific sites were identified and replaced with mutant and wild-type CSE protein, showed altered H_2Sproduction. E339A mutant demonstrated 6-fold enhancement in H_2S production.[82] This HEK 293 cells based model was selected for endogenous H_2S detection using our fluorescent probe.

3.2 Materials and Methods

3.2.1 Materials and Instruments

The experiments were performed with analytical grade reagents. Otherwise stated, all chemicals were purchased from Sigma-Aldrich Chemical Company (St Louis, MO) and used without further purification. Ultrapure water (18.2 MΩ˙cm) was used from a Millipore water purification system. BODIPY based Cu(II)-cyclen complex fluorescent probe (probe 3) was gifted by Dr. Wu Haixia.[77] Slow H_2S releasing compounds GYY 4137 and FW1010 were gifted by Dr. Deng Lih-Wen.[78,79] Fluorescence measurements were carried out using a Synergy HT microplate fluorescence reader from Bio-Tek Instruments Inc., (Winooski, Vermont), installed with KC4 software and Tecan Ultra 384 Micro plate reader. Fluorescence spectra were obtained on PerkinElmer LS55 fluorometer with slit width at 10 nm for both excitation and emission. Cellular 3-D and 2-D images were captured using Olympus IX 81, Fluroview FV1000 confocal microscopy equipped with a 60X water lens. Further the images were processed using IMARIS 3.0 (BITPLANE AG) and imageJ software.

3.2.2 Cell culture

The Mouse leukaemic macrophage cells (RAW 264.7) from the American Type Culture Collection (ATCC, Manassas, VA, USA) were cultured in

DMEM (Dulbecco's modified Eagle's medium, GIBCO Grand Island, NY, USA) with 10% fetal bovine serum (FBS, Hyclone), 1% glutamine(GIBCO), 100 U/mL streptomycin (GIBCO) and 100 μg/mL penicillin (GIBCO).The cells were maintained at 37 ^{o}C in a 5% CO_2 humidified environment. The Human Embryonic kidney 293 (HEK 293) cells and Michigan Cancer Foundation-7 (MCF-7) cells were gifted by Dr. Deng Lih-Wen and cultured in DMEM (Dulbecco's modified Eagle's medium) with 10% fetal bovine serum, 1% glutamine, 100 U/mL streptomycin, 100 μg/mL penicillin at 37 ^{o}C and 5% CO_2 humidified environment. Eppendorf centrifuge (5804R) equipped with a F-34-6-38 rotor was utilised for passaging and supernatant separation. RAW 264.7 cells were selected due to the previously observed stability during liposome mediated probe delivery. MCF-7 cells were previously utilized in synthetic polysulfide treatment for their activity against cancer cells. Lastly, HEK 293 cells were identified for their high transfection ratio, stable during gene knock down and overexpression.

3.2.3 Encapsulation of probe 3 in DOTAP liposome

DOTAP (28 μl, 25 mg/ml in chloroform) and probe 3 (42.4 μl, 1 mg/mL or 645 μM in dichloromethane) were taken in a glass vial. The solvent was evaporated using a stream of argon. The resulting lipid film was further dried under vacuum for 20 mins to remove the traces of chloroform. The lipid film was hydrated with 1ml of de-ionized water and sonicated for 10 min to give clear solution of liposome with DOTAP and probe 3 concentrations at 1.0 mM and of 100 μM respectively. The probe- DOTAP mixture (1:10) was protected from light and stored in ice. It was further diluted to 10 μM and 100 μM using

DMEM to obtain the working concentrations.

3.2.4 in-vitro toxicity profile of the BODIPY based Cu(II) cyclen fluorescent probe

The in-vitro toxicity of probe 3 was measured using CytoTOX96 non-radioactive cytotoxicity assay kit (Promega, Madison, WI, USA). RAW 264.7 cells were seeded at 2 x 10^4 cells/well in a 96 well Flat bottom plate (Corning Glass Works, Corning, NY,USA) and incubated overnight in DMEM with 10% fetal bovine serum at 37^{o}C and 5% CO2 humidified environment. 0.1 mg of Probe 3 was dissolved in equal volume of dichlormethane – DMSO (1:1)(42.4 μL,1.0 mg/ml), which was further diluted to the working concentration (1μM-50μM) using DMEM and added to the respective culture wells. Cells cultured in DMEM without probe 3 being added served as low control. The Culture plate was incubated for 4 hours at 37^{o}C and 5% CO_2 humidified environment. The spontaneous LDH (lactate dehydrogenase) release was measured by performing the LDH assay as prescribed the manufacturer on the media supernatant. Triton X-100 was added to the wells to determine maximum LDH release in individual wells. The 96-well plate was centrifuged at 1000 x g for 10 mins to separate the cell debris. The absorbance was measured at 490 nm using Tecan Ultra 384 Micro plate reader. The cytotoxicity was expressed as the percentage between the result of the spontaneous LDH and that of the maximum LDH from the same time.

3.2.5 Intra-cellular detection of exogenous H_2S using probe 3

The RAW 264.7 cells cultured in 10mm cell culture plates were centrifuged and the pellet was re-dissolved in 1ml fresh DMEM for transfer. For confocal imaging, the cell suspension was transferred to chambered

coverglass (Lab-Tek chambered #1.0 borosilicate cover glass system) at $6x10^3$ cells/well and incubated for 24 h. The probe-DOTAP mixture was further diluted to 10.0 μM using DMEM. RAW264.7 cells were cultured in chambered cover glass for 24 hours were washed with PBS thrice and treated with probe 3 in DOTAP liposome solution (10.0 μM) for 2 h. The excess probe 3- DOTAP solution in the wells was removed by washing the cells with PBS. The cells were then treated with Na_2S dissolved in DMEM (25 μM) for 30 minutes and then washed with PBS three times followed by addition of fresh cell culture media. The non-Na_2S treated cells served as the control and cells treated with glutathione (GSH, 2mM) and L-cysteine (Cys, 2mM) after probe 3-DOTAP treatment served to test the selectivity of the probe towards H_2S in biological system. The intracellular localization of probe 3 was investigated by a sequential Z-step scanning using confocal microscopy (Olympus IX 81, Fluroview FV1000) equipped with a 60X water lens. Probe was excited with a 650 nm Ar laser, and the fluorescent images were collected using filter sets selective above 680 nm wavelength. Images were processed in IMARIS 3.0 (BITPLANE AG) software.

3.2.6 Analysis of dose dependent increase in fluorescent intensity inside the cells.

The cell suspension after passage was transferred to chambered coverglass (Lab-Tek chambered #1.0 borosilicate cover glass system) at $6x10^3$ cells/well and incubated for 24 h. The probe-DOTAP mixture was further diluted to 10.0 μM using DMEM. RAW264.7 cells were cultured in chambered cover glass for 24 hours were washed with PBS thrice and treated with probe 3 in DOTAP liposome solution (10.0 μM) for 2 h. The excess probe 3- DOTAP solution in

the wells was removed by washing the cells with PBS. The cells were then treated with Na_2S dissolved in DMEM (25, 50, 100, 150 and 200 μM) for 30 min and then washed with PBS three times followed by addition of fresh cell culture media. The non-Na_2S treated cells served as the control. The 2D images were captured using confocal microscopy (Olympus IX 81, Fluroview FV1000) equipped with a 60X water lens. Probe was excited with a 650 nm Ar laser, and the fluorescent images were collected using filter sets selective above 680 nm wavelength. FluroviewImages were processed in IMARIS 3.0 (BITPLANE AG) software.

The 2-D images captured using confocal microscopy in the same sample but at different location were organized using imageJ software to obtain the fluorescent intensity curve. The average intensity of the negative control and different treatments has to be determined to obtain the fluorescence emitted by the cells alone. Each sample was analyzed at (n = 8) different locations to obtain the fluorescent intensity and corresponding no. of cells present within the given area.

$$Average\ Intensity = \frac{Fluorescent\ intensity\ within\ \ the\ area}{No.\ of cells\ present}$$

To obtain statistically significant dose response curve, the average intensity values of the samples were correlated to the concentration of Na_2S added.

3.2.7 Detection of H_2S released by polysulfides in MCF-7 cells

The MCF-7 cell suspension after passage was transferred to chambered coverglass (Lab-Tek chambered #1.0 borosilicate cover glass system) at $6x10^3$ cells/well and incubated for 24 h. The probe-DOTAP mixture was further diluted to 10.0 μM using DMEM. RAW 264.7 cells were cultured in chambered cover glass for 24 hours were washed with PBS thrice and treated

with probe 3 in DOTAP liposome solution (10.0 μM) for 2 h. The excess probe 3- DOTAP solution in the wells was removed by washing the cells with PBS. The cells were treated with diallyl disulfide (DADS, 100, 200μM) and diallyl trisulfide (DATS, 100, 200 μM) and incubated for 20 min prior to confocal imaging. The treatment procedure is clearly explained in Table 3.1.

Table 3.1 Treatment pattern of poly sulfides after addition of probe 3- DOTAP solution in 8-chambered coverglass.

Negative Control	100μM DADS	200μM DADS	GSH+200μM DADS
400μM NaHS	100μM DATS	200μM DATS	GSH+200μM DATS

Two sample in chambered coverglass receiving 200μM DADS treatment were pre-stimulated using GSH (1mM) for 2h before the probe treatment to aid the polysulfide breakdown and increase the yield of H_2S inside the cells. The sample with probe 3 - DOTAP treatment alone served as the negative control. The sample with 400µM of NaHS treatment served as the positive control for comparing the maximal releasing potential of the synthetic polysulfides.

Prior to imaging under microscope the cells were washed with PBS and transferred to fresh DMEM. The 2D images were captured using confocal microscopy (Olympus IX 81, Fluroview FV1000) equipped with a 60X water lens. Probe was excited with a 650 nm Ar laser, and the fluorescent images were collected using filter sets selective above 680 nm wavelength. FluroviewImages were processed in IMARIS 3.0 (BITPLANE AG) software.

3.2.8 Image based analysis of slow H_2S-releasing compounds

The MCF-7 cell suspension after passage was transferred to chambered coverglass (Lab-Tek chambered #1.0 borosilicate cover glass system) at $2x10^3$ cells/well and incubated for 24 h. The cells were first treated with GYY4137

(4-methoxyphenyl(morpholino) phosphinodithiolate) and FW1010 (4-methoxyphenyl phosphinodithiolate) to undergo the slow releasing of H_2S into the cells. The chambered coverglass was treated with GYY 4137 (400 μM, 800 μM) and FW 1010 (400 μM, 800 μM) for 36 h and transferred to CO_2 incubator. The chamber without any treatment was maintained to check for cell death during incubation and imaging. The treatment procedure is clearly explained in Table 3.2. After the incubation, the cells were washed with PBS thrice and treated with probe 3 in DOTAP liposome solution (10.0 μM) for 2 h. The excess probe 3- DOTAP solution in the wells was removed by washing the cells with PBS. NaHS (100 μM, 200 μM, 400 μM) was added to the chambers without any pre-treatment acted as positive control and washed

Table 3.2 Treatment pattern of slow H_2S-releasing compounds after addition of probe 3- DOTAP solution in 8-chambered coverglass.

Negative Control	400μM FW	400μm GYY	200μM NaHS
100μM NaHS	800μM FW	800μM GYY	400μM NaHS

with PBS thrice after 30 mins. The sample with probe 3- DOTAP solution alone served as negative control. The NaHS treatment (100 μM, 200 μM, 400 μM) served as the standard H_2S release profile for understanding the releasing potential of slow releasing compounds.

The 2D images were captured using confocal microscopy (Olympus IX 81, Fluroview FV1000) equipped with a 60X water lens. Probe was excited with a 650 nm Ar laser, and the fluorescent images were collected using filter sets selective above 680 nm wavelength. FluroviewImages were processed in IMARIS 3.0 (BITPLANE AG) software. The fluorescent intensity was quantified in (n=5) different sample of the same treatment using imageJ

software in order to compare the amount of H_2S released by slow releasing molecules and the spontaneously releaser such as NaHS. The fluorescent intensity was correlated to the concentration to obtain a statistically significant curve.

3.2.9 Detection of endogenous H_2S by over-expression of CSE in HEK 293 cells

HEK293 cells were transfected with CSE-specific siRNA (Sense: 5'-CCUGUGAAGAUCAAAUCUUdTdT-3'; Antisense:5'-AAGAUUUGAUCUUCACAGGdTdT-3') using Lipofectamine RNAiMAX (Invitrogen) according to manufacturer's protocol. After 8 hour of siRNA transfection, plasmids encoded for either wild-type (WT) or E339A CSE mutant were transfected with calcium phosphate transfection method.[82] Transfected cells were incubated in 37 °C, 5% CO_2 incubator for 36 hours then subjected to imaging procedures.

The cells were transferred in chambered glass plate 24 h prior to the imaging. The cells were treated with probe 3 in DOTAP liposome solution (10.0 μM) for 1 hour and excess probe 3-DOTAP mixture in the wells were removed by washing the cells with PBS. The intracellular localization of probe in cells was determined confocal microscopy (Olympus IX 81, Fluroview FV1000) equipped with a 60X water lens. Probe was excited with a 650 nm Ar laser, and the fluorescent images were collected using filter sets selective above 680 nm wavelength. Images were processed in IMARIS 3.0 (BITPLANE AG) software.

3.3 Results and discussion

3.3.1 In-vitro toxicity profile

The *in vitro* cytotoxicity of probe 3 on RAW 264.7 cells was measured using CytoTOX96 non-radioactive cytotoxicity assay kit (Promega, Madison, WI, USA). The fluorescent probe was distributed at different concentrations(1μM- 50μM) and LDH assay was performed. The cytotoxicity of the probe 3 at the working concentration 10μM in cellular imaging studies showed negligible toxicity (less than 2%). (Fig 3.3)

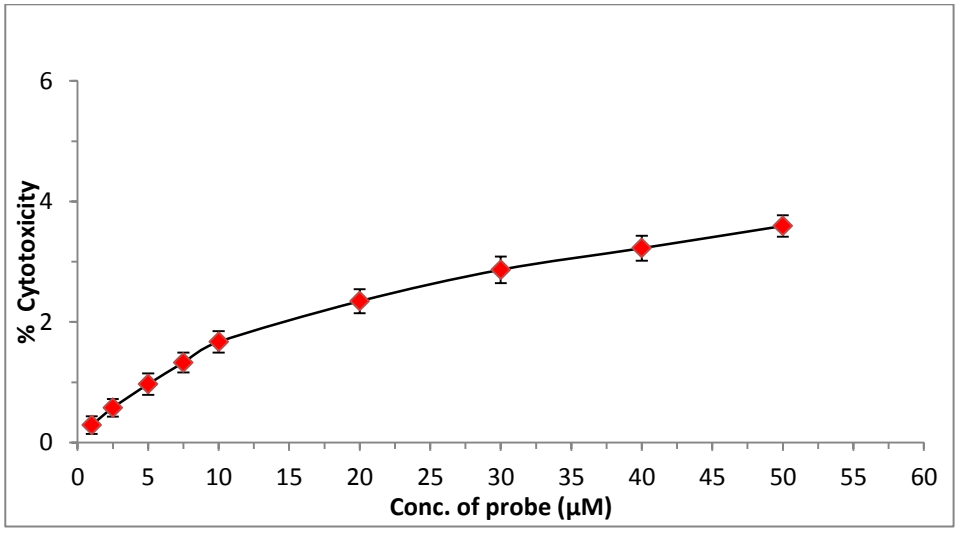

Figure 3.3 Cytotoxicity data for probe 3 at various concentrations after 4 h incubation with RAW 264.7 cells. The concentration of probe at 10μM adopted in the cell imaging experiment demonstrates negligible cytotoxicity (less than 2%).

3.3.2 Exogenous H_2S detection in RAW 264.7 cells

The BODIPY based Cu(II)-cyclen complex fluorescent probe (probe 3) was encapsulated with DOTAP liposome for detection for of exogenous H_2S generated by Na_2S (25 μM) dissolved in DMEM. The low concentration of Na_2S was preferred to achieve maximum sensitivity inside the cellular environment. The non- Na_2S treated cells served as the control for distinguishing the fluorescent intensity increase after Na_2S treatment. The

selectivity of the probe inside the cellular membrane is challenged by the presence of other thiol containing biomolecules such as cysteine and glutathione (GSH). The higher concentration of both cysteine (2 mM) and GSH (2 mM)

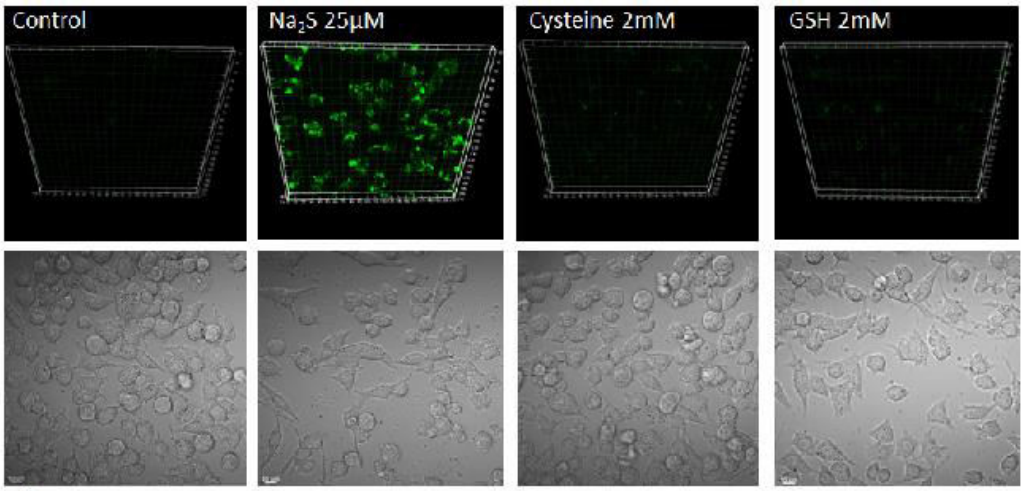

Figure 3.4 Detection of H_2S in RAW 264.7 cells. The probe 3(10 μM) in RAW 264.7 was specifically turned on by H_2S contributed by Na_2S (25 μM) but not the other thiol-containing molecules such as cysteine (2 mM) or glutathione (2 mM).

were tested simultaneously to observe fluorescent change by interacting molecules. 3-D fluorescent images of the Na_2S treatment revealed the localization of probe in cytoplasm and the regions of H_2S generation with bright fluorescent spots when compared to the control (Figure 3.4). On the other hand, the GSH and cysteine treatment showed no change in fluorescent intensity and was comparable to the control (Figure 3.4). The 2-D white field images in the lower panel of Figure 3.4 clearly shows the morphology of the cell and healthy elongated RAW 264.7 cells. The sensitivity and selectivity of the probe towards H_2S was clearly established in the cellular environment using 3-D imaging. The 2-D imaging coupled with quantitative analysis of fluorescent intensity will confirm the detection limit of the NIR based H_2S biosensor.

3.3.3 Fluorescent intensity based dose-response plot

The confocal microscopy based imaging studies gives a clear idea on the cellular structures, organelles and interactions. The advent of fluorescent probe mediated imaging studies opened up a completely new environment of intracellular interactions, cellular signaling cascades and florescent tagging. Most of the fluorescent probes reported for cellular imaging of gaseous molecules, reactive oxygen species, proteins projects only the recognition of the molecule of interest. The quantification of the molecule of interest inside the cellular environment compliments the qualitative imaging and provides a the complete details in the cytoplasm. The approach of image based fluorescent intensity analysis would enable us to understand the intracellular behavior of H_2S. The fluorescent imaging was carried for the various exogenously treated (0, 25, 50, 100, 150 and 200μM of Na_2S) RAW 264.7 cells. The 2D images were taken at different cellular pockets of the same treatment to enable error free curve. The 2D fluorescent images of the different concentrations of H_2S showed sequential increase in fluorescent intensity ranging from of 25 to 200μM.(Figure 3.5) The marked increase in fluorescent intensity was quantified using imageJ software. The fluorescent intensity values with respect to the no. of cell present in the cellular pocket were correlated to the concentration of Na_2S with statistical significance. It is also to be noted that the H_2S levels in media is not detectable after 1.5 h after addition of Na_2S. The uptake of H_2S by the cells is subject to the availability in the media and will be less than the concentration added. The sensitivity of the probe inside the cell gives a clear idea of H_2S levels

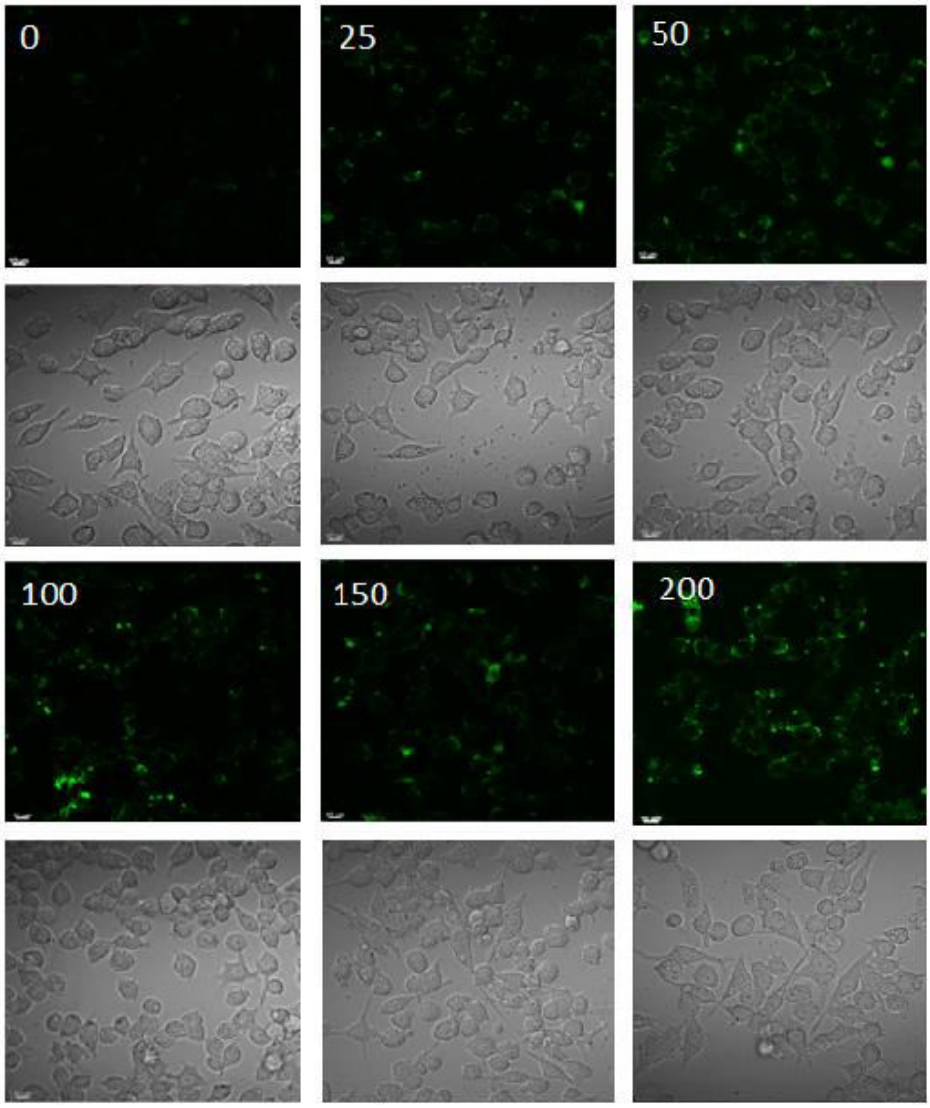

Figure 3.5 Exogenous H_2S detection in RAW 264.7 cells by probe 3. The upper panel is the fluorescent images and lower panel is corresponding bright field images. The cells were treated with probe 3 in DOTAP liposome (10 μM) for 1 hour and Na_2S(0, 25, 50, 100, 150 and 200μM) for 30min respectively. The images were quantified using imageJ for dose response of H_2S concentration and fluorescence intensity (n = 12).

under various treatment with the reference values, the various natural and synthetic H_2S donating compounds can be screened. The image based quantification can also be applied in understanding the various interactions of H_2S in physiological and pathological conditions. The NIR property of the probe makes it suitable for animal imaging studies to unravel the role of H_2S in different organs. The cardioprotective role of H_2S can be further elucidated with *in vitro* and *in vivo* studies.

3.3.4 H_2S releasing profile of Polysulfide compounds

Polysulfide compounds are naturally occurring allium plant species and abundant donor of H_2S in the presence of glutathione (GSH). The MCF-7 cells were treated with commercially available polysulfides: Diallyl disulfide (DADS), diallyl trisulfide (DATS). The 2-D imaging was carried out in order to understand the releasing capacity of the polysulfides, which can be further utilized as reference for other higher chain polysulfide compounds. The half-life of both the polysulfides were within 30 mins and their H_2S generating capacity was monitored in the presence and absence of GSH. GSH acts as a reducing agent in breaking down the long chain polysulfides into H_2S. Polysulfides can be potent hydrogen sulfide donor and can be utilised in various avenues such as anticancer, cardioprotective, vasoactive and neuronal functioning.[83] The non-treated cells and cell treated with probe 3-DOTAP solution followed by NaHS (400 μM) served as low and high control to of H_2S availability in cells. The 2-D imaging of DADS treatment showed increase in fluorescent intensity compared to the non-treated sample but lower than the high control.(Figure 3.6) In order to aid the polysulfide breakdown GSH

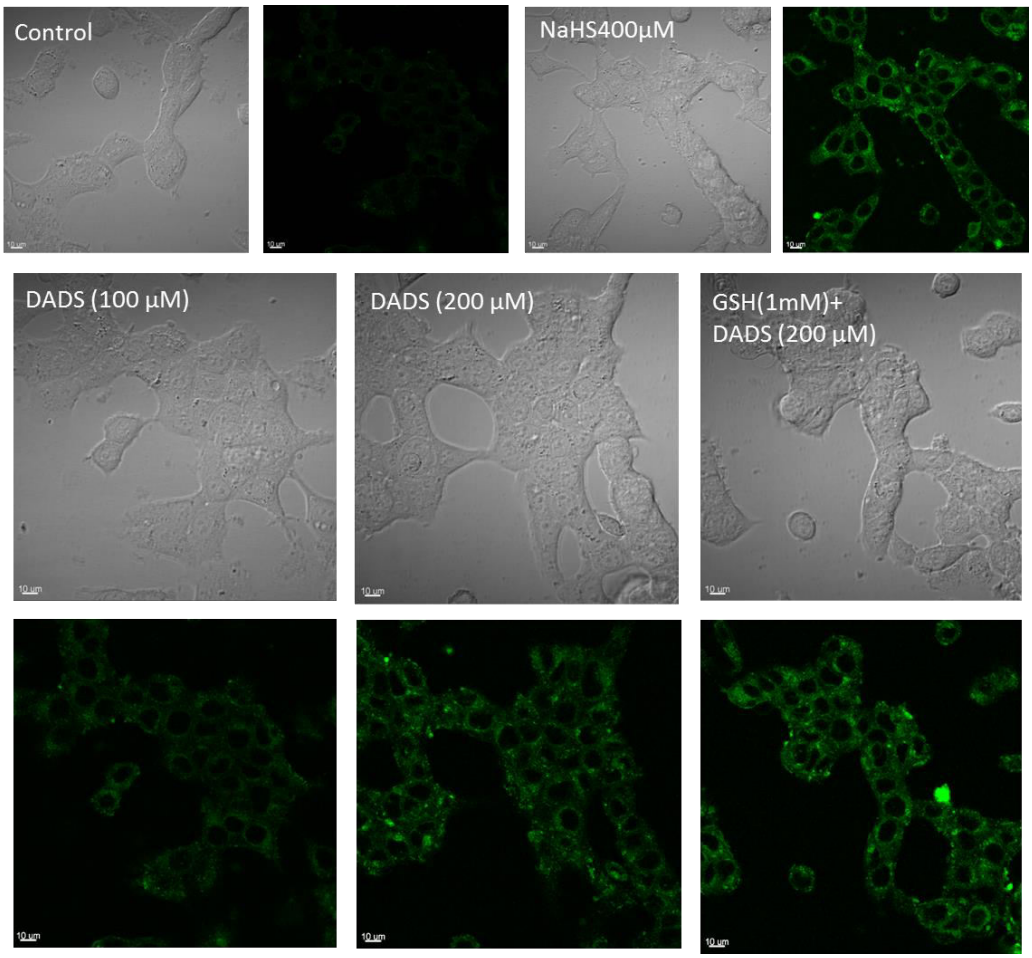

Figure 3.6 Fluorescent and corresponding bright field images of diallyl disulphide treatment in MCF-7 cells. The cells were treated with probe 3 in DOTAP liposome followed by NaHS 400 μM, DADS 100 μM, DADS 200 μM and GSH 1mM + DADS 200 μM. Non-treated cells acted as control.

(1 mM) pre-treatment followed by DADS treatment had marked increase in fluorescent intensity, suggesting the breakdown of DADS into H_2S by GSH. It is also to be noted that DADS releasing high concentration of H_2S in short span of time could have deleterious effect on the cells. The DATS treatment also showed similar change in fluorescent intensity when compared with low control. The fluorescent intensity change between pre-treated GSH and without pre-treatment had minimum change.(Figure 3.7) However, the fluorescent intensity increase was comparable to the high control.

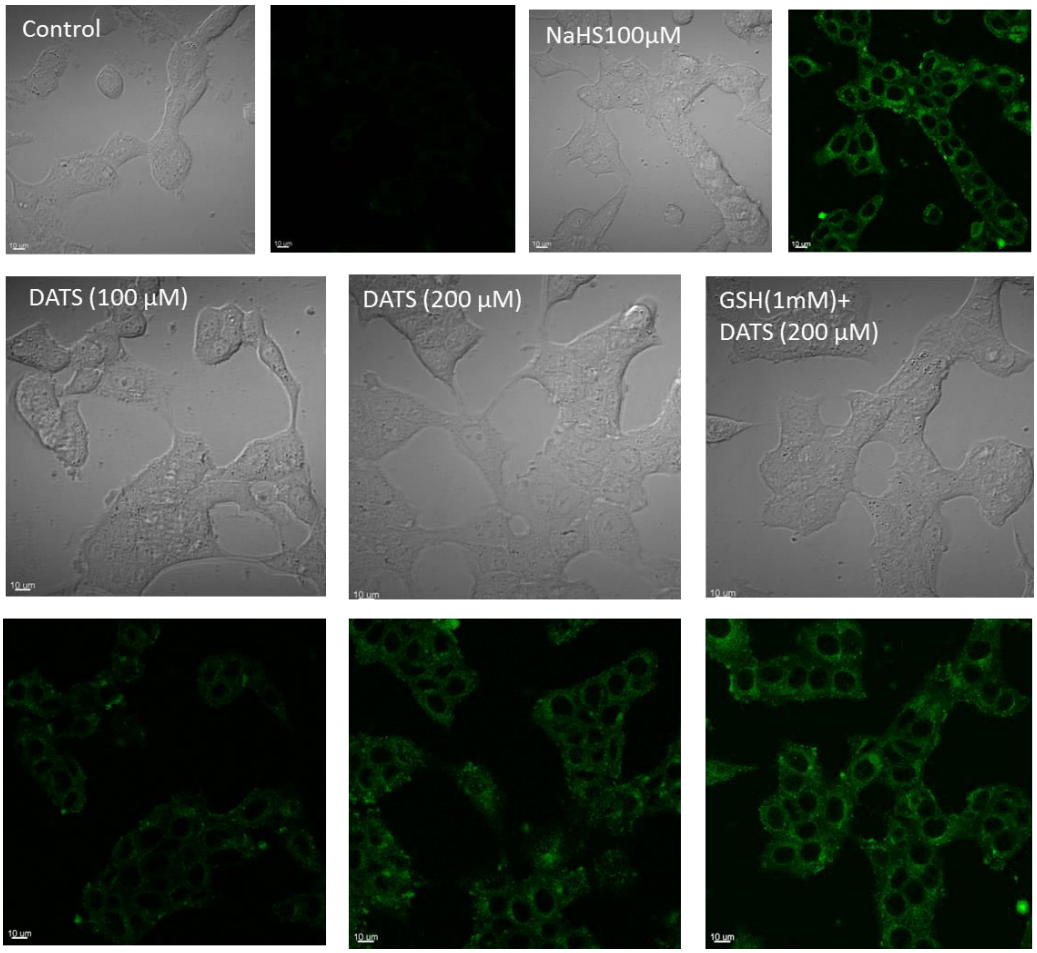

Figure 3.7. Fluorescent and corresponding bright field images of diallyl trisulfide (DATS) treatment in MCF-7 cells. The cells were treated with probe 3 in DOTAP liposome followed by NaHS 400 μM, DATS 100 μM, DATS 200 μM and GSH 1mM + DATS 200 μM. Non-treated cells acted as control.

The preliminary analysis of H_2S releasing capacity by basic polysulfide compounds using fluorescent imaging proved to be an viable application of near infrared BODIPY based Cu(II)-cyclen complex fluorescent probe.

3.3.5 Cellular localization of H_2S released by slow H_2S releasing compounds

The slow- H_2S releasing compounds are currently getting recognized for anti-cancer therapy due to their ability to cease the proliferation of tumor cells. The anti-proliferative effect exhibited by these compounds is associated only with the cancer cells and normal cells are left unaffected. The prolonged

exposure of tumor cells to H_2S (> 3 days) causes altered glucose metabolism and pH homeostasis leading pH disruption induced cell death.[80,81]

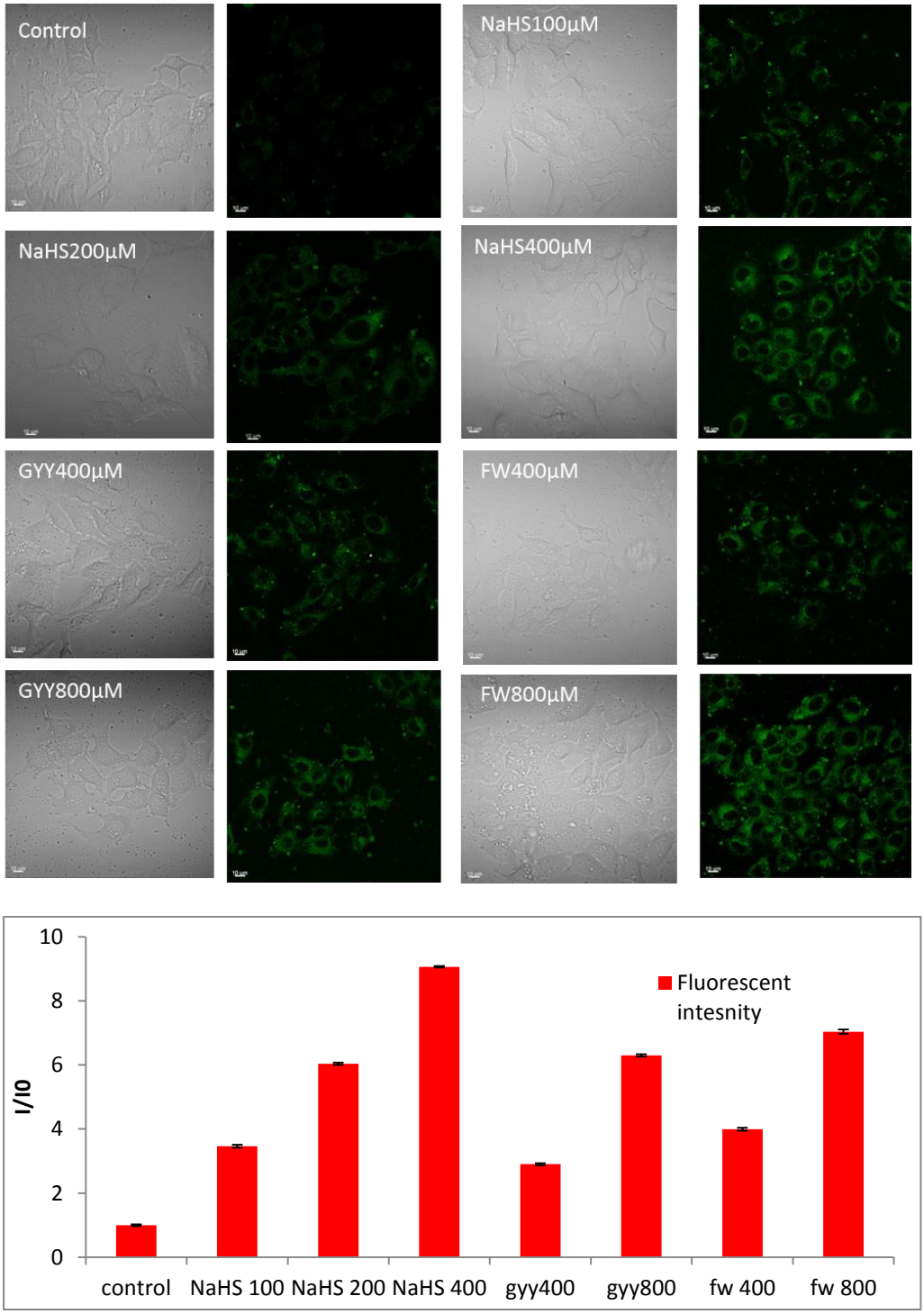

Figure 3.8. Fluorescent and corresponding bright field images of GYY 4137 and FW 1010 treatment in MCF-7 cells. The cells were treated with probe 3 in DOTAP liposome followed by NaHS (100, 200 and 400 μM) GYY4137 (400 μM, 800 μM) and FW1010 (400 μM, 800 μM) Non-treated cells acted as control. The images were quantified using imageJ for fluorescence intensity plot(n = 10).

MCF-7 cells were treated with GYY 4137 and FW 1010 compounds at two concentrations (400 μM, 800 μM) for 36 hour followed by probe 3-DOTAP treatment. 2D images were captured after the incubation time and marked increase in fluorescent intensity was observed. To determine the exact concentration of intracellular H_2S, NaHS treatment (100, 200 and 400 μM) was carried out simultaneously. The fluorescent intensity was quantified using imageJ software and the values were plotted in a fluorescent intensity plot. The slow- H_2S releasing compounds were also quantified by identifying different cellular pockets of the same treatment(Figure 3.8). The fluorescent intensity plot clearly elucidated the H_2S releasing potential when compared to the control group as there was statistically significant increase in the fluorescence intensity.

On comparison with the control, both GYY 4137 and FW 1010 at 400 μM had a 4-fold increase in fluorescent intensity, whereas at 800 μM it showed 6-fold increase in fluorescent intensity (Figure 3.8). The releasing potential of these compounds at their respective concentration was also compared to the standard NaHS. This clearly established that at 400 μM, the fluorescence intensity detected was similar to that of 100 μM NaHS and at 800 μM, the fluorescence intensity detected was similar to that of 200 μM. Image based quantification proved to be a vital tool in order to interpret the high quality images with solid quantitative evidence. The working concentration of slow H_2S releasing compounds can act as a pivotal information in designing anti-cancer drugs and treatments.

3.3.6 Detection of endogenously produced H_2S by over expressed CSE mutant

The fluorescent probe was successfully applied in various exogenously generated H_2S avenues, exhibiting high sensitivity and selectivity towards the molecule of interest. The endogenously generated H_2S in the presence of cystathionine-γ-lyase (CSE) enzyme and cysteine substrate was also analyzed

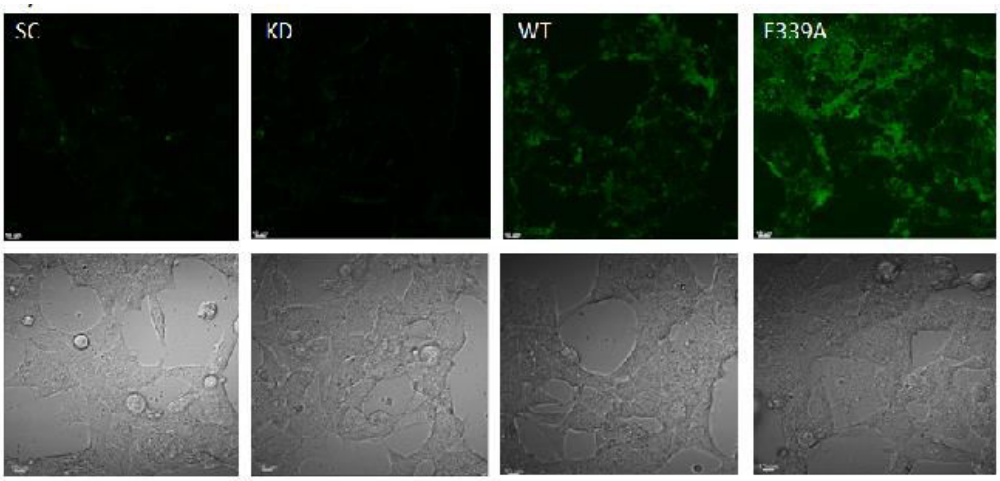

Figure 3.9. Fluorescence microscopy pictures showing signals in cells with manipulated expression of endogenous H_2S-producing enzymes, cystathionine-γ lyase (CSE). Overexpression of wild-type (WT) CSE in HEK293 cells showed increased fluorescence intensity as compared to scrambled control (SC) and CSE knock-down (KD). Hyperactive E339A mutant showed even enhanced fluorescence signal than WT.

to extend the sensitivity of probe 3. HEK293 cells after siRNA-gene silencing and plasmid overexpression of cystathionine-γ-lyase (CSE) proved to be a viable model for live cell monitoring of endogenously generated H_2S. The increase in fluorescent intensity was observed in cells with the overexpression of wild-type (WT) CSE (transfection efficiency of nearly 70%). (Figure 3.9) Interestingly, overexpression of a hyperactive CSE mutant, E339A showed even higher fluorescence intensity as compared to WT.[82] This demonstrates that the probe is sensitive enough to detect the endogenous H_2S produced by overexpressed CSE proteins. It is not surprising that there was no obvious

difference between the fluorescence signals of scrambled control (SC) and CSE knock-down (KD) cells. The probe is unable to distinguish the minor change in fluorescent intensity due to production of H_2S below the basal level.

3.4 Conclusion

To outline, BODIPY based Cu(II)-cyclen complex fluorescent probe (probe 3) was applied in various cellular environment to assess the selectivity and sensitivity. The exogenous H_2S generated by Na_2S and NaHS in RAW264.7 and MCF- 7 cells were qualitatively and quantitatively measured with the fluorescent probe. The application of image based analysis to address the *in vitro* H_2S concentrations and fluorescent intensity values obtained were utilized in developing dose-response curve. The intracellular quantification would act as reference during screening of natural and synthetic H_2S generating compounds. Polysulfides slated as the future in cardioprotective and functional food arena was screened to give a preliminary idea on their releasing profiles. On the other hand, detection and quantification of slow- H_2S releasing compounds could act as a possible anti-cancer therapeutics. Another important application is the detection of low micromolar endogenous H_2S generated by overexpression of CSE in HEK 293 cells promotes the sensing activity of the fluorescent probe. The intracellular interaction of H_2S with biological targets and regulatory molecules can be monitored under high resolution microscopy. The radical scavenging activity of H_2S is still under consideration due to the difficulty in understanding the regeneration of H_2S with relevance to the basal requirement for physiological functioning. Finally, BODIPY based Cu(II)-cyclen complex fluorescent probe was applied in various experimental conditions to understand the H_2S metabolism and physiological role.

Chapter 4. Image based analysis of intracellular NO_2-H_2S interaction

4.1 Introduction

The gasotransmitters exhibit mutual interaction among themselves for eliciting various signalling pathways and metabolic processes. Previous reports suggest that NO donor drugs enhanced H_2S production and increased CSE expression in cultured smooth muscle cells. Similar to the release of NO by acetylcholine, release of H_2S by NO adds a line of essential evidence for the physiological role of H_2S. [84]

The integrated vascular effect of H_2S and NO may not be a simple algebraic summation of their individual actions observed that the vasorelaxant effect of sodium nitroprusside (SNP), a NO donor, was enhanced by incubating rat aortic tissues with 30 μM NaHS. In a different study, pre-treating aortic tissues with 60 μM H_2S inhibited the vasorelaxant effect of SNP. This discrepancy may be partially explained by the experimental conditions of these studies, including differences in tissue preparations and tension development before the application of H_2S. It is also to be noted that H_2S may interact with NO and its oxidation products to form an unidentified nitrosothiol moiety, which is physiologically inactive but further breaks down to form nitroxyl which has various physiological effects such as vascular regulation, radical scavenging and cardioprotection. [85,86,88,92]

The interaction between H_2S and NO oxidation products would be pivotal in understanding their regulation of physiological effects. The fluorescent probes that are selective for individual compounds of interest were applied simultaneously for live cell monitoring. The DOTAP liposome based delivery method was preferred for delivery of fluorescent probesand LPS stimulated

NO production was favoured to monitor the interaction with H_2S generated by exogenous donors.

4.2 Materials and Methods

4.2.1 Materials and Instruments

The experiments were performed with analytical grade reagents. Otherwise stated, all chemicals were purchased from Sigma-Aldrich Chemical Company (St Louis, MO) and used without further purification. Ultrapure water (18.2 MΩ˙cm) was used from a Millipore water purification system. Cellular 3D and 2D images were captured using Olympus IX 81, Fluroview FV1000 confocal microscopy equipped with a 60X water lens. Further the images were processed using IMARIS 3.0 (BITPLANE AG) and imageJ software.

4.2.2 Cell culture

The mouse leukaemic macrophage cells (RAW 264.7) from the American Type Culture Collection (ATCC, Manassas, VA, USA) were cultured in DMEM (Dulbecco's modified Eagle's medium, GIBCO Grand Island, NY, USA) with 10% fetal bovine serum (FBS, Hyclone), 1% glutamine, 100 U/mL streptomycin and 100 μg/mL penicillin. The cells were maintained at 37 ^{o}C and 5% CO_2 humidified environment. Eppendorf centrifuge (5804R) equipped with a F-34-6-38 rotor was utilised for passaging and supernatant separation.

4.2.3 Encapsulation of H_2S and NO_2 sensitive fluorescent probes in DOTAP liposome

DOTAP (28 μl, 25 mg/mL in chloroform), Rhodamine-B containing nickel(II) dithiocarbamate complex (probe 2) (40.2 μl, 1 mg/ml or 645 μM in dichloromethane) and BODIPY based Cu(II)-cylen complex (probe 3) (42.4

μL, 1 mg/ml or 645 μM in dichloromethane) were taken in a glass vial. The solvent was evaporated using a stream of argon stream. The resulting lipid film was further dried under vacuum for 20 mins to remove the traces of chloroform. The lipid film was hydrated with 1mL of de-ionized water and sonicated for 10 min to give clear solution of liposome with DOTAP(1mM) probe 2 (30μM) and probe 3 (50μM). The combined probe- DOTAP mixture was protected from light and stored in ice. It was further diluted to DOTAP(100μM) probe 2 (30μM) and probe (5μM) using DMEM to obtain the working concentration.

4.2.4 Cellular toxicity of combined H_2S-NO_2 fluorescent probe

The combination of probe 2 and probe 3 was evaluated for cytotoxicity using CytoTOX96 non-radioactive cytotoxicity assay kit (Promega, Madison, WI, USA). RAW 264.7 cells were seeded at 2 x 10^4 cells/well in a 96-well flat bottom plate (Corning Glass Works, Corning, NY,USA) and incubated for overnight in DMEM (Dulbecco's Modified Eagle Medium) with 10% fetal bovine serum at 37 ^{o}C and 5% CO_2 humidified environment.

Probe 2 was weighed at 0.1 mg and dissolved in equal volume of dichloromethane - DMSO (40.2 μl, 1.0 mg/ml). Similarly probe 3 was weighed at 0.1 mg and dissolved in equal volume of dichloromethane - DMSO (42.4 μL, 1.0 mg/ml).The two vials were mixed together and further diluted to the working concentration (1μM- 50μM) using DMEM and added to the culture wells. Cells cultured in DMEM without any treatment served as low control. The Culture plate was incubated for 4 h at 37 ^{o}C and 5% CO_2 humidified environment. The spontaneous lactate dehydrogenase (LDH) release was measured by performing the LDH assay as prescribed the manufacturer on the

media supernatant. Triton X-100 was added to the wells to determine maximum LDH release in individual wells. The 96-well plate was centrifuged at 1000 g for 10 min to separate the cell debris. The absorbance was measured at 490 nm using Tecan Ultra 384 Micro plate reader. The cytotoxicity was expressed as the percentage between the result of the Spontaneous LDH and that of the maximum LDH from the same time.

4.2.5 Simultaneous monitoring of intracellular H_2S and NO_2 using fluorescent probe

The RAW 264.7 cells cultured in 10mm cell culture plates were centrifuged and the pellet was re-dissolved in 1 mL fresh DMEM for transfer. For confocal imaging, the cell suspension was transferred to chambered coverglass (Lab-Tek chambered #1.0 borosilicate cover glass system) at $6x10^3$ cells/well and incubated for 24 h. RAW 264.7 cells were cultured in chambered cover glass for 12 h were washed with PBS and stimulated with LPS (2 μg/ml) in DMEM for 16 h. After stimulation the cells were bathed with PBS thrice and treated combined probe-DOTAP mixture was diluted to DOTAP(100 μM) probe 2 (30 μM) and probe (5 μM) using DMEM. After the incubation, RAW264.7 cells were washed with PBS thrice and treated with combined probe in DOTAP liposome solution for 2 h. The excess combined probe- DOTAP solution in the wells was removed by washing the cells with PBS. The cells were then treated with Na_2S dissolved in DMEM (25 μM) for 30 mins and then washed with PBS three times followed by addition of fresh cell culture media. The combined probe- DOTAP treatment alone served as the negative control. LPS pre-stimulated cells followed by combined probe-DOTAP treatment served as positive control for NO_2 monitoring. Whereas

sequential treatment of LPS, fluorescent probe and Na2S (100 μM) were utilized for simultaneous monitoring. The fluorescent probe treatment followed by Na_2S (100 μM) served as positive control for H_2S localization.

Table 4.1 Treatment pattern of slow H_2S-releasing compounds after addition of combined probe - DOTAP solution in 8-chambered coverglass.

Probe alone	Probe + LPS (2μg/ml)	Probe + Na_2S (100 μM)
Probe + LPS (2 μg/ml) + Na_2S (50 μM)	Probe + LPS (2 μg/ml) + Na2S (100 μM)	Prob e+ LPS(2 μg/ml) + Na2S (200 μM)

The intracellular localization of fluorescent probe was investigated by a sequential z-step scanning using confocal microscopy (Olympus IX 81, Fluroview FV1000) equipped with a 60X water lens. Probe was excited with a 650 nm Ar laser, and the fluorescent images were collected using filter sets selective above 680 nm wavelength. Images were processed in IMARIS 3.0 (BITPLANE AG) software.

4.2.6 Time based scan of cellular H_2S and NO_2 environment

The RAW 264.7 cells cultured in 10 mm cell culture plates were centrifuged and the pellet was re-dissolved in 1ml fresh DMEM for transfer. For confocal imaging, the cell suspension was transferred to chambered coverglass (Lab-Tek chambered #1.0 borosilicate cover glass system) at $6x10^3$ cells/well and incubated for 24 h. RAW 264.7 cells were cultured in chambered cover glass for 12 h were washed with PBS and stimulated with LPS (2 μg/ml) in DMEM for 16 h. After stimulation the cells were bathed with PBS thrice and treated combined probe-DOTAP mixture was diluted to DOTAP(100 μM) probe 2 (30 μM) and probe (5 μM) using DMEM. After the incubation, RAW264.7 cells

were washed with PBS thrice and treated with combined probe in DOTAP liposome solution for 2 h. The excess combined probe - DOTAP solution in the wells was removed by washing the cells with PBS. The combined probe-DOTAP treatment alone served as the negative control. LPS pre-stimulated cells followed by combined probe- DOTAP treatment served as positive control for NO_2 monitoring. The fluorescent probe treatment followed by Na2S (100 μM) served as positive control for H_2S localization. The sample after sequential treatment of LPS, fluorescent probe was kept under the microscope for time-based scan. Na_2S (100 μM) was added to the well and time based sequential scanning was selected for continuous monitoring the of fluorescent intensity changes.

The intracellular localization of fluorescent probe for sensing H_2S was investigated using confocal microscopy (Olympus IX 81, Fluroview FV1000) equipped with a 60X water lens. Chamberglass was excited with a 650 nm Ar laser, and the fluorescent images were collected using filter sets selective above 680 nm wavelength. Fluorescence specific to NO_2 was observed with an excited 540 nm Ar laser, and the images were collected using filter sets more than 560 nm. Images were processed in IMARIS 3.0 (BITPLANE AG) software.

4.3 Results and discussion

4.3.1 In-vitro toxicity profile

The *in vitro* cytotoxicity of combined probe on RAW 264.7 cells was measured using CytoTOX96 non-radioactive cytotoxicity assay kit (Promega, Madison, WI, USA). The fluorescent probe was distributed at different concentrations (1- 50μM) and LDH assay was performed.

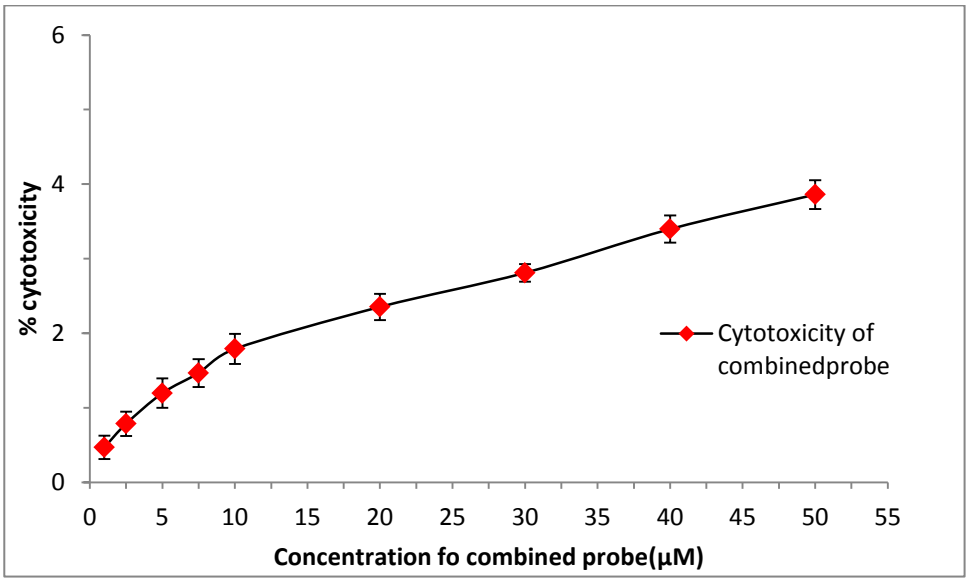

Figure 4.1 Cytotoxicity data for combined probe at various concentrations after 4 h incubation with RAW 264.7 cells. The concentration of probe adopted in the cell imaging experiment demonstrates negligible cytotoxicity (less than 2%).

The cytotoxicity of the combined probe at the working concentration cellular imaging studies showed negligible toxicity (less than 2%). (Figure 4.1)

4.3.2 Intracellular monitoring of H_2S and NO_2.

The successful application of Rhodamine-B derived nickel(II) dithiocarbamate complex(probe 2) in live cell monitoring of NO_2 and BODIPY based Cu(II)-cyclen complex fluorescent probe (probe 3) in intracellular localization of H_2S allowed us to work on the simultaneous monitoring. The two hydrophobic fluorescent probes with vast difference in the wavelength of operation proved to be an ideal candidate for understanding the H_2S and NO_2 interactions. The 3D imaging of non-treated cells, LPS pre-stimulated cells and Na_2S in the presence of combined probe- DOTAP solution acted as the blank and positive controls respectively (Figure 4.6). The sequential treatment of LPS pre-stimulation followed by combined probe in DOTAP solution and Na_2S (200 μM)(Figure 4.2c) served as the sample to be monitored.

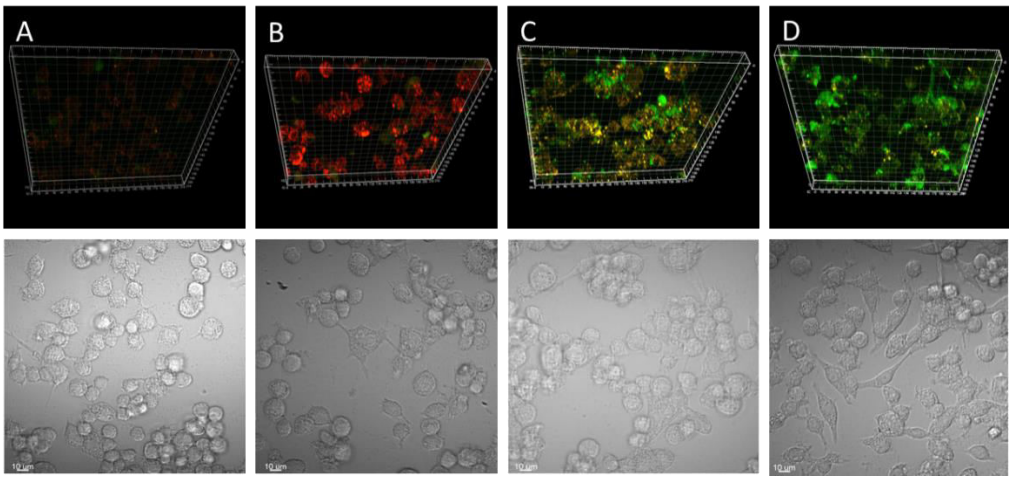

Figure 4.2. Fluorescent imaging of NO_2-H_2S by combined probe-DOTAP mixture. The upper panel is fluorescent images and the lower panel is corresponding bright-field images. Cells a) treated with DOTAP- combined probe solution for 2 hours b) pre-stimulated with LPS (2 μg/ml) for 16 hours and treated with combined probe solution for 2 hours. c) Sequentially treated with LPS (2 μg/ml) for 16 hours, DOTAP- combined probe solution for 2 hours and Na_2S(200 µM) for 30 min. d) incubated with DOTAP- combined probe solution for 2 hours and Na_2S (200 µM) for 30 min.

and Na_2S in the presence of combined probe- DOTAP solution acted as the blank and positive controls respectively (Figure 4.2). The sequential treatment of LPS pre-stimulation followed by combined probe in DOTAP solution and Na_2S (200 µM)(Figure 4.2c) served as the sample to be monitored. The fluorescent intensity increase was prevalent when individual positive controls(Figure 4.2b and 4.2d) were compared with blank suggesting that individual working mechanism of probe was not affected. However, during sequential treatment in the presence of both the laser source, the fluorescence at the same cellular sample was analyzed to unravel any possible interactions between the two biomolecules. The LPS pre-stimulated RAW 264.7 cells were followed by 3 different Na_2S (50, 100 and 200 μM) treatments to observe the physiological changes. In figure 4.3c, 4.3d, 4.3e (red fluorescence represents NO_2 and green fluorescence represents H_2S), the NO_2 fluorescence signal intensity takes a dip with the increase in H_2S concentration as observed

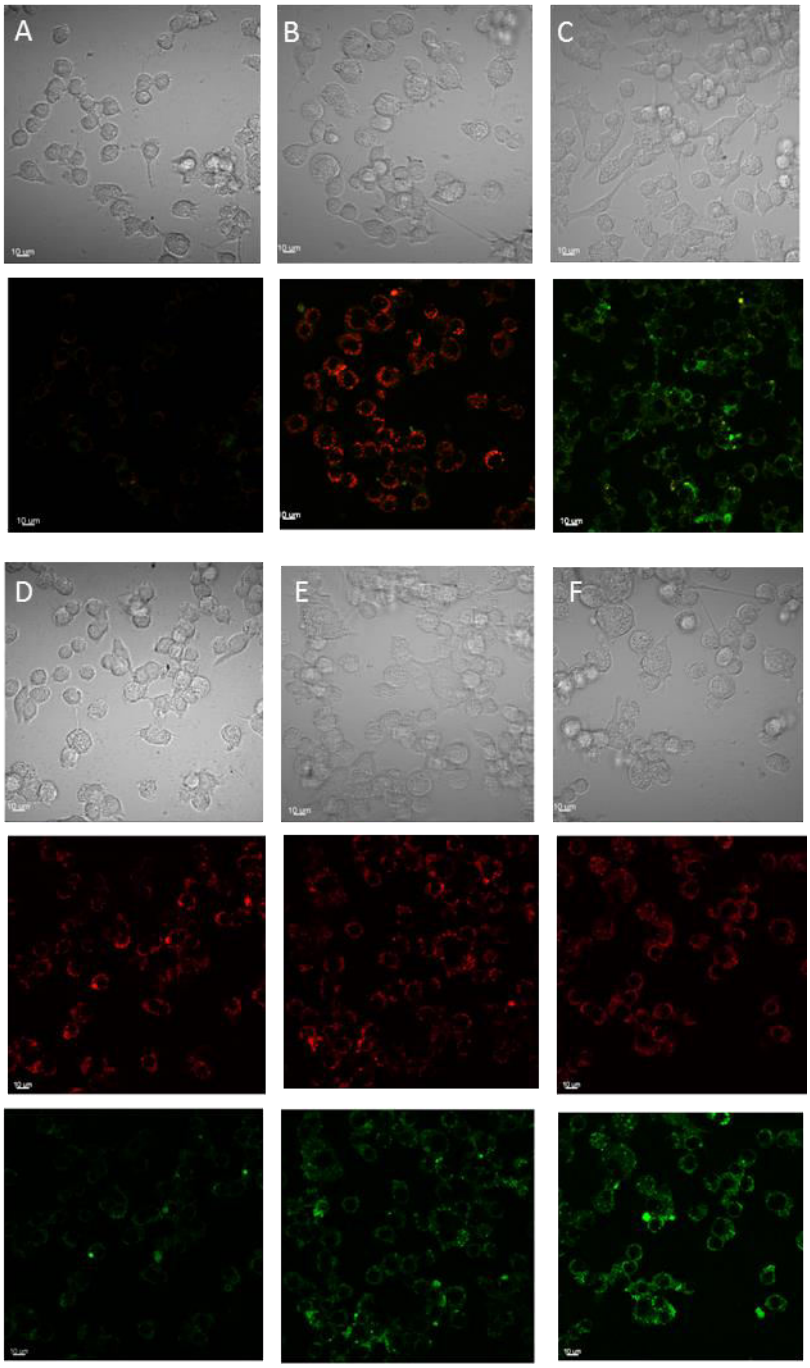

Figure 4.3 Fluorescent and corresponding bright field images of NO_2-H_2S in RAW 264.7 cells. The cells were a) treated with DOTAP- combined probe solution for 2 hours. b) pre-stimulated with LPS (2 μg/ml) for 16 hours and treated with combined probe solution for 2 hours. c) DOTAP- combined probe solution for 2 hours and Na_2S (200 μM) for 30 min. d) H_2S and NO_2 images are separately monitored in sequential treatment of LPS (2 μg/ml) for 16 hours, DOTAP- combined probe solution for 2 hours and Na_2S(50 µM), e) Na_2S(100 μM), f) Na_2S(200 μM) for 30 min.

in the intensity change suggesting the prevalence of both the gaseous molecules. This interaction was further analyzed under individual laser

sources. The reduction in NO_2 fluorescent intensity can be attributed to the inhibitory effect of H_2S on NOS expression leading to reduction in NO levels. It is premature to come to a conclusion due to the experimental conditions but the reduction in fluorescent intensity relevant to NO_2 after the addition of H_2S is evident. Another possible explanation is the formation of or nitroxyl (HNO) pronotnated form of NO. The highly reducing nature of H_2S can directly react with NO or oxidation intermediates of NO to form HNO. Biologically less known nitrosothiol (HSNO) can be chemically formed which may further react with other thiols to release HNO.[89,91] The time based scan would reveal the potential of exogenous H_2S on LPS induced NO and its oxidative products generation.

4.3.3 Time-based Scanning of H_2S and NO_2 inter-talk

The time-based scan was performed to monitor the changes after the hydrogen sulfide treatment to the RAW 264.7 cells. The chambered glass containing LPS activated macrophages were treated with combined probe in DOTAP solution was mounted in the confocal microscopy sample chamber. The Addition of H_2S was followed by 2-D imaging at every 15 min interval . In figure 4.4a, 4.4b, 4.4c are blank, positive control for NO_2 and positive control for H_2S respectively act as standard for comparing the sequential treatment of NO_2 and H_2S . The time based scan of NO_2 fluorescent intensity revealed a minor decrease in fluorescence (Fig. 4.4d) with time whereas the H_2S fluorescent intensity had a sequential increase(Fig. 4.4e). The fluorescent intensity across the H_2S time span observed to be incremental. The NO_2-H_2S interactions inside the cell are evident but longer interval of time and presence of slow-

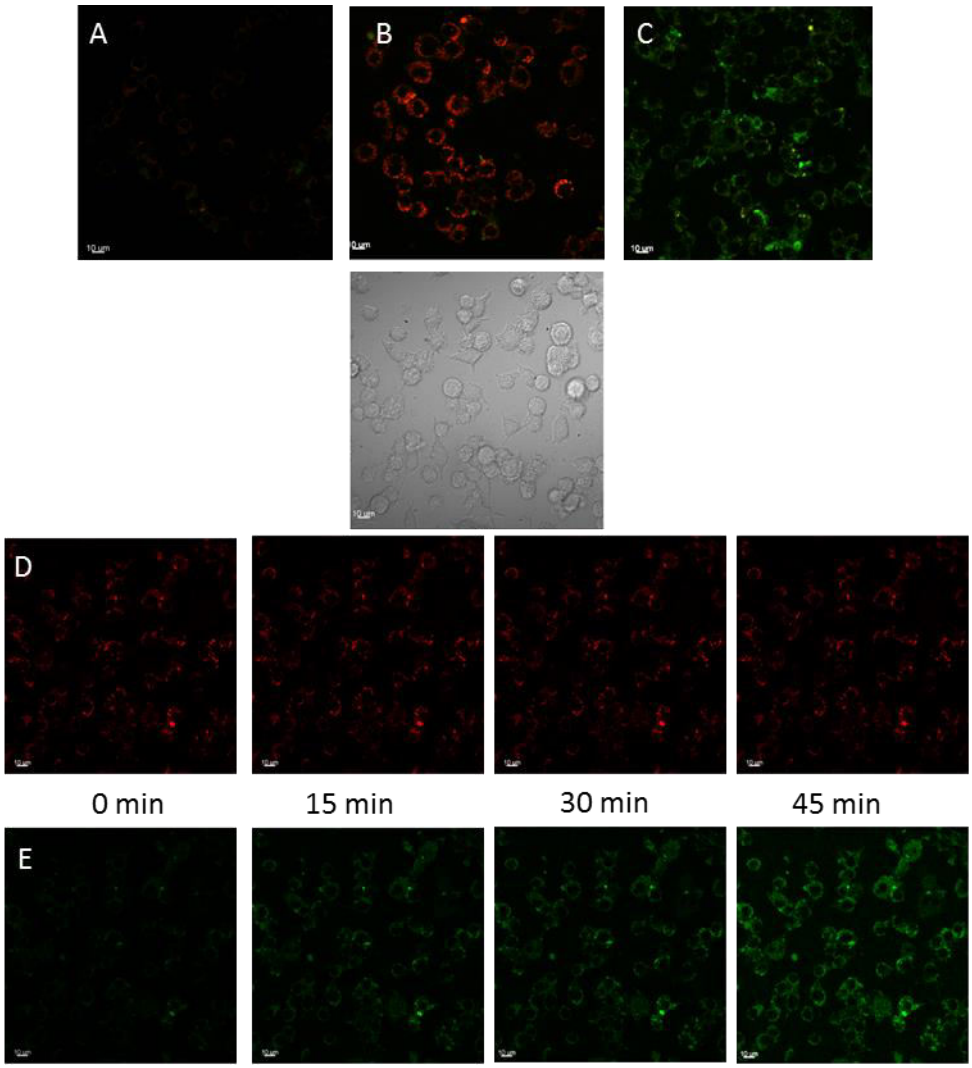

Figure 4.4 Fluorescent and corresponding bright field images of time based scanning of NO_2- H_2S intertalk in RAW 264.7 cells. The cells were a) treated with DOTAP- combined probe solution for 2 hours. b) pre-stimulated with LPS (2 μg/ml) for 16 hours and treated with combined probe solution for 2 hours. c) DOTAP- combined probe solution for 2 hours and Na_2S(200 μM) for 30 mins. d) under NO_2 laser slit alone open followed by sequential treatment with LPS (2 μg/ml) for 16 hours, DOTAP- combined probe solution for 2 hours and Na_2S(200 μM) for 30 mins. e) under the H_2S laser slit alone open and same treatment as d).

H_2S releasing compound would enable to understand the mutual interactions. It is also to be noted that the liposome containing two different fluorophores had no interaction and achieved maximum detection. The qualitative imaging was carried out simultaneously on the intracellular NO_2- H_2S level and further quantitative intensity analysis would warrant the interactions.

4.4 Conclusion

In summary, the DOTAP liposome can be utilised for delivering hydrophobic moieties without affecting the cellular physiology. The combination of NO_2- H_2S sensitive fluorescent probes were encapsulated and successfully delivered into the cells. The concentration based analysis of H_2S regulating the endogenous NO_2 production was evident. Possible interaction between oxidation products of NO and H_2S was observed with decrease in fluorescent intensity. The time based scan showed the rapid generation of H_2S within the cell with minor interactions between the two molecules. It is to be noted that the nitric oxide and hydrogen sulfide interact to form biologically inactive nitrosthiols.

4.5 Future work

The liposomes based delivery can be extended in delivering various hydrophobic molecules into the cells to understand their activity in physiological conditions. The rhodamine B derived nickel(II) dithiocarbamate complex probe sensitive to NO_2 can be applied simultaneously with other radical sensing fluorescent probes to understand the chemistry behind ROS and RNS formation. With the help of NO sensitive biosensor the fate of NO and its interconversion with oxidation products can be explored. The quantitative image based analysis can be applied in reference to the images obtained using microscopy. The synthetic NO releasing compounds can be screened *in vitro* to determine whether NO is released or the oxidation products of NO. The concentration dependent activity of NO in physiological processes can be discussed in detail in relevance to the oxygen rich cellular environment converts it to NO_2 or N_2O_3. The NO_2 sensitive fluorescent probe

can be used as a viable tool in ageing related cellular damage which is directly related to the ROS and RNS production. Endogenous NO_2 acts as the primary defense against invading microbes suggesting a possible application in immunity and inflammation.

BODIPY based Cu(II)-cyclen complex fluorescent probe due to its near infra -red region of emission, it serves as potent animal imaging fluorescent probe. The physiological levels of H_2S can be quantified with the aid of high quality imaging techniques. The cardioprotective and neuroprotective ability of H_2S can be taken to the next step of functional food development. The interaction between the gaso-transmitters in regulating various signaling and metabolic pathways can be unearthed.

Quantitative evidence would warrant the claims of possible NO_2- H_2S interaction inside the cells. The antioxidant role of H_2S could be confirmed if radical scavenging ability against NO_2 or other RNS by formation of biologically less known nitrosothiol.

References

1. Olson, K. R.; Donald, J. A. *Acta Histochem.,* **2009,** 244.

2. Schulz, R.; Kelm, M.; G. Heusch, G. *Cardiovasc. Res.,* **2004**, 61, 402.

3. Hosoki, R.; Matsuki, N.; Kimura, V; *Biochem. Biophys. Res. Commun.,* **1997**, 237, 527.

4. Furchgott, R. F.; Zawadzki, J. V. *Nature,* **1980**, 288, 373–376.

5. Marks, G. S.; Brien, J. F.; Nakatsu, K. ; McLaughlin, B. E. *Trends Pharmacol. Sci*, **1991**, 12, 185.

6. Abe, K. ; Kimura, H. *J Neurosci.,* **1996**, 16, 1066.

7. Wu, L.; Wang, R. *Pharmacol. Rev.,* **2005**, 57, 585.

8. Paradise, W. A.; Vesper, B. J.; Goel, A.; Waltonen, J. D.; Altman, K. W.; Haines, G. K.; Radosevich, J. A. *Int. J. Mol. Sci.*, **2010**, 11, 2715.

9. Eto, K.; Asada, T. ; Arima, K. ; Makifuchi, T.; Kimura, H. *Biochem. Biophys. Res. Commun.,* **2002**, 293, 1485.

10. Haldane, J. B. *Biochem. J.*, **1927**,21,1068.

11. Palmer, R. M. J.; Ferrige, A. G.; Moncada, S. *Nature,* **1987**, 327, 524.

12. Alderton, W. K.; Cooper, C. E.; Knowles, R. G. *BiochemJ*., **2001**, 357, 593.

13. Conner, E.M.; Grisham, M. B. *Enzymol.*, **1995**, 7, 3.

14. Moncada, S.; Palmer, R. M. J; Higgs, E. A. *Pharmacol. Rev.,* **1991**, 43,109.

15. Radi, R.; Beckman, J. S.; Bush K. M.; Freeman, B. A. *Arch. Biochem. Biophys.*, **1991**, 288, 481.

16. Zelickson, B.R.; Ballinger, S. W.; Dell'Italia, L. J.; Zhang J.; Darley-Usmar, V.M. *In Encyclopedia of Biological Chemistry*, Academic Press, **2013**, 17.

17. Marletta, M. A.; Yoon, P. S.; Iyengar, R.; Leaf, C. D.; Wishnok J. S. *Biochemistry,* **1988**, *27*, 8706.

18. Ischiropoulos, H.; Zhu, L. Beckman, J. S. *Arch. Biochem. Biophys.*, **1992**, 298, 446.

19. Szabo, C. *Nat. Rev. Drug Discov.,* **2007**, 6, 917.

20. Bian, J. S., Yong, Q. C.; Pan, T. T.; Feng, Z. N.; Ali, M. Y.; Zhou, S.; Moore, P. K. *J. Pharmacol. Exp. Ther*., **2006**, 316, 670.

21. Qu, K.; Lee, S. W.; Bian, J.S.; Low, C.M.; Wong, P. T. *Neurochem. Int.*, **2007**, 52, 155.

22. Dombkowski, R. A.; Russell, M. J.; Schulman, A.A.; Doellman, M.M.; Olson, K.R. *Am. J. Physiol. Regul. Integr. Comp. Physiol*., **2005**, 288, 243.

23. Singh, S.; Banerjee, R. *Biochim. Biophy. Acta (BBA) - Proteins and Proteomics*, **2011**, 11, 1518.

24. Calvert, J. W.; Coetzee, W. A.; Lefer, D. J. *Antioxid. Redox Signal*, **2010**, 12, 1203.

25. Shibuya, N.; Tanaka, M.; Yoshida, M.; Ogasawara, Y.; Togawa, T.; Ishii, K.; Kimura, H. *Antioxid. Redox Signal*, **2009**,11, 703.

26. Hetrick, E. M.; Schoenfisch, M. H. *Annu. Rev. Anal. Chem.*, **2009**, 2, 409.

27. Ishigami, M.; Hiraki, K.; Umemura, K.; Ogasawara, Y. Ishii, K.; Kimura, H. *Antioxid. Redox Signal.*,**2009**, 12, 205.

28. Lee Y.; Kim, J. *Anal. Chem.*, **2007**, 79, 7669.

29. Kumar N.; Bhalla, V; Kumar M. *Coord. Chem. Rev.,* **2013**, 257, 2335.

30. Lakowicz, J.R. Principles of fluorescence spectroscopy 3rd ed., Springer, New York , 2006.

31. Kojima, H.; Nakatsubo, N.; Kikuchi, K.; Kawahara, S.; Kirino, Y.; Nagoshi, H.; Hirata, Y.; Nagano T. *Anal. Chem*., **1998**, 70, 2446.

32. McQuade L. E.; Lippard S. J. *Curr. Opi. Chem. Bio.*, **2010**, 14, 43.

33. Gabe, Y.; Urano, Y.; Kikuchi, K.; Kojima, H.; Nagano T. *J. Am. Chem. Soc.*, **2004**, 126, 3357.

34. Sasaki, E.; Kojima, H.; Nishimatsu, H.; Urano, Y.; Kikuchi, K.; Hirata, Y.; Nagano T. *J. Am. Chem. Soc.*, **2005**, 127, 3684.

35. Izumi, S.; Urano, Y.; Hanaoka, K; Terai, T.; Nagano T. *J. Am. Chem. Soc*., **2009** , 131, 10189.

36. Zheng, H.; Shang, G. O.; Yang, S. Y.; Gao, X.; Xu. J. G. *Org. Lett.*, **2008**, 10, 2357.

37. Lim, M. H.; Xu, D.; Lippard, S. J.; *Nat. Chem. Biol.*, **2006**, 2, 375.

38. Ouyang, J.; Hong, H.; Shen, C.; Zhao, Y. ; Ouyang, C. G.; Dong, L.; Zhu, J. H.; Guo, Z.J.; Zeng, K.; Chen, J. N. *Free Radical Biol. Med.*, **2008**, 28, 1426.

39. Gomes, A.; Fernandes, E.; Lima, J. *J. Fluoresc*., **2006**, 16, 119.

40. Wardman, P. *Free Radic. Bio. Med.*, **2007**, 23, 995.

41. Yang, D.; Wang, H. L.; Sun, Z. N.; Chung, N. W.; Shen J. G. *J. Am. Chem. Soc*., **2006**, 128, 6004.

42. Z.N. Sun, H.L. Wang, F.Q. Liu, Y. Chen, P.K.H. Tam, D. Yang, *Org. Lett.*, **2009**, 11, 1887.

43. Lin, V. S.; Chang, C. J. *Curr. Opin. Chem. Bio.*, **2012**, 16, 595.

44. Lippert, A. R.; New, E.J.; Chang, C.J. *J. Am. Chem. Soc*., **2011**, 133, 10078.

45. Peng, H.; Cheng, Y.; Dai, C.; King, A. L.; Predmore, B. L.; Lefer, D.J.; Wang, B. *Angew. Chem. Int.*, **2011**, 50, 9672.

46. Yu, F. ; Li, P. ; Song, P.; Wang, B.; Zhao, J.; Han, K. *Chem. Commun.*, **2012**, 48, 2852.

47. Montoya, L. A.; Pluth, M.D.; *Chem. Commun*., **2012**, 48, 4767.

48. Chen, S.; Chen, Z. J.; Ren, W.; Ai, H. W. *J. Am. Chem. Soc.*, **2012**, 134, 9589.

49. Das, S. K.; Lim, C. S.; Yang, S. Y.; Han, J.H.; Cho, B.R. *Chem. Commun.*, **2012**, 48, 8395.

50. Qian, Y.; Karpus, J.; Kabil, O.; Zhang, S.Y.; Zhu H. L.; Banerjee, R.; Zhao, J. He, C. *Nat. Commun.*, **2011**, 2, 495.

51. Qian, Y.; Zhang, L.; Ding, S.; Deng, X.; He, C.; Zheng, X. E.;. Zhu, H. L.; Zhao, J.*Chem. Sci.*, **2012**, 3, 2920.

52. Liu, C.; Pan, J.; Li, S.; Zhao, Y.; Wu, L. Y.; Berkman, C. E.; Whorton, A. R.; Xian, M. *Angew. Chem. Int. Ed.*, **2011**, 50, 10327.

53. Liu, C.; Li, S.; Peng, B.; Whorton, A. R.; Xian, M. *Org. Lett.*, **2012**, 14, 2184.

54. Sasakura, K.; Hanaoka, K.; Shibuya, N.; Mikami, Y.; Kimura, Y.; Komatsu, T.; Ueno, T.; Terai, T.; Kimura, H.; Nagano, T. *J. Am. Chem. Soc.*, **2011**, 133, 18003.

55. Hou, F.; Huang, L.; Xi, P.; Cheng, J.; Zhao, X.; Xie, G.; Shi, Y.; Cheng, F.; Yao, X.; Bai, D.; Zeng, Z. *Inorg. Chem.*, **2012**, 51, 2454.

56. Hou, F.; Cheng, J.; Xi, P.; Chen, F.; Huang, L.; Xie, G.; Shi, Y.; Liu, Y.; Bai, D.; Zeng, Z. *Dalton Trans.*, *2012*, 41, 5799.

57. Laurent, M.; Johannin, G.; Guyader, H.; Fleury, A. *Biology of the Cell*, **1992**, 76, 113.

58. Jackson, W.; Yamada, M; Moninger, Y.; Grose, C. *Journal of Virological Methods*, **2013**, 193, 244.

59. Marley N. A.; Gaffney J. S. White R. V.; Rodriguez C. L.; Herndon S. E.; Dunlea E.; Volkamer R. M.; Molina L. T.; Molina M. J. *Rev. Sci. Instrum.,* **2004**, *75*, 4595.

60. Das A.; Dost R.; Richardson T.; Grell, M.; Morrison J. J.; Turner M. L. *Adv. Mater.,* **2007**, *19*, 4018.

61. Hogarth G. *Mini-Rev. Med. Chem.,* **2012**, *12*, 1202.

62. Mohamed G. G.; Ibrahim N. A.; Attia, H. A. E. *Spectrochim. Acta A,* **2009**, 72, 610.

63. Jiang, L. J.; Luo, Q. H.; Wang, Z. L.; Liu D. J.; Zhang Z.; Hu H. W. *Polyhedron,* **2001**, 20, 2807.

64. Yordanov N. D.; Iliev V.; Shopov D. *Inorg. Chim. acta,* **1982**, 60, 17.

65. Hongtao L.V.; Shubiao Z.; Bing W.; Shaohui C.; Jie, W. *Journal of Controlled Release*, **2006**, 114, 100.

66. Srinivas R.; Samanta S.; Chaudhuri A. *Chem. Soc. Rev.,* **2009**, *38*, 3326.

67. Chen W. S.; Yan, W. L.; Huang, L. *Cancer Immunol. Immun.,* **2008**, 57, 517.

68. Hesterberg, T. W.; Bunn W. B.; McClellan R. O.; Hamade A. K., Long C. M.; Valberg P. A. *Crit. Rev. Toxicol.,* **2009**, *39*, 743.

69. Eiserich, J. P. Hristova, M.; Cross, C. E.; Jones, A. D.; Freeman, A.; Halliwell, B.; van der Vliet, A. *Nature,* **1998**, *391*, 393.

70. Augusto, O.; Bonini, M. G.; Amanso, A. M.; Linares, E.; Santos C. X.; De Menezes, S. L. *Free Radical Bio. Med.,* **2002**, *32*, 841.

71. J. E. Saavedra, J. E.; Dunams, T. M.; Anderson, J. L. F.; Keefer, L. K. *J. of Org. Chem.,* **1992**, *57*, 6134.

72. Nagano, T. *J. Clin. Biochem. Nutr*., 2009, 45, 111.

73. Marletta, M. A. *J. Med. Chem*., 1994, 37, 1899.

74. Lewis, R. S.; Tannenbaum, S. R.; Deen, W. M. *J. Am. Chem. Soc.,***1995**, *117*, 3933.

75. Lewis, R. S.; Tamir, S.; Tannenbaum S. R.; Deen W. M. *J. Biol. Chem.,* **1995**, *270*, 29350.

76. Yan, Y.; Krishnakumar, S.; Yu, H.; Ramishetti, S.; Deng, L. W.; Wang, S.; Huang L.; Huang D. *J. Am Chem Soc*, **2013**, *135*, 5312.

77. Haixia, W.; Krishnakumar S.; Jie, Y.; Dong, L.; Hongyi, Q.; Lee, Z. W.; Deng, L. W.; Huang, D. *Chem. Asian J.,* 9, 3604.

78. Ku D. D.; Abdel-Razek T. T.; Dai, J.; Kim-Park S.; Fallon, M. B.; Abrams, G. A. *Clin. Exp. Pharm. and Physi.*, **2002,** 29, 84.

79. Lee, Z. W.; Zhou, J.; Chen, C. S.; Zhao, Y.; Tan, C. H. *PLoS ONE*, **2011**, 6, e21077.

80. Liao, L. L.; Tsai, C. T.; Atan M. S.; Lee, Z. W.; Deng, L.W.; Dymock, B. W.; Feng, W.; Tan, C. H.; Moore, P. K. *Nitric Oxide*, **2013**, 31, 47.

81. Lee, Z. W.; Tay, Y. W.; Tan, C.; Hagen, T.; Moore, P. K.; Deng, L.W. *Nitric Oxide*, **2013**, 31, 27.

82. Huang, S.; Chua, J. H.; Yew, W. S.; Sivaraman, J.; Moore, P. K.; Tan, C. H.; Deng, L. W. *J. Mol. Biol.* **2010,** *396,* 708.

83. Gloria, A.; Giuseppe, L.; Robert, W.; Hetal, D.; Scott, T.; Rakesh, P.; Victor, M.; Darley, U.; Jeannette, E.; David, W. *Proc. Natl. Acad. Sci. USA,* **2007**, 104,17977.

84. Elrod, J. W.; Calvert, J. W.; Morrison, J.; Doeller, J. E.; Kraus, D. W.; Tao, L. *Proc. Natl. Acad. Sci. USA,* **2007**, 104, 15560.

85. Pan, T. T.; Feng, Z. N.; Lee, S. W.; Moore, P. K.; Bian, J. S. *J. Mol. Cell Cardiol.*, **2006**, 40, 119.

86. Minamishima, S.; Bougaki, M.; Sips, P.; Yu, J. D.; Minamishima, Y. A.; Elrod, J. W. *Circulation,* **2009**;120, 888.

87. Yong, Q. C.; Hu, L. F.; Wang, S.; Huang, D.; Bian, J. S. *Cardiovasc. Res.,* **2010**, 88, 482.

88. Whiteman, M.; Li, L.; Kostetski, I.; Chu, S. H.; Siau, J. L.; Bhatia, M.; Moore, P. K. *Biochem. Biophys. Res. Commun.*, **2006**, 343, 303.

89. Elrod, J. W.; Calvert, J. W.; Morrison, J.; Doeller, J. E.; Kraus, D. W.; Tao L. *Proc. Natl. Acad. Sci. USA,* **2007**, 104, 15560.

90. Fernanda, V.; Fernando, N.; Paulo R. V. *Arq. Bras. Cardiol.,* **2000**, 74, 4.

91. Irvine, J. C; R. H.; Ritchie, J. L.; Favaloro, K. L.; Andrews, R. E.; Widdop, B. K.; Kemp-Harper. *Trends in Pharm.Sci.,* **2008**, 29, 601

92. Wang, R. *FASEB J.*, **2002**, 16, 1792.

93. Leventis. R.; Silvius J. R. *Biochim. Biophys. Acta.,* **1990**, 1023, 124.